

Constrained Control using Convex Optimization

by

John Marc Shewchun

B.A.Sc. Aerospace Engineering
University of Toronto, 1995

Submitted to the Department of Aeronautics and Astronautics
in partial fulfillment of the requirements for the degree of

Master of Science in Aeronautics and Astronautics

at the

MASSACHUSETTS INSTITUTE OF TECHNOLOGY

August 1997

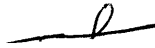
September 1997

© Massachusetts Institute of Technology 1997. All rights reserved.

Author

Department of Aeronautics and Astronautics

August 8, 1997



Certified by

Eric Feron

Assistant Professor

Thesis Supervisor



Accepted by

Jaime Peraire

Associate Professor

Chairman, Department Graduate Committee

MASSACHUSETTS INSTITUTE OF TECHNOLOGY

OCT 15 1997

LIBRARIES

Constrained Control using Convex Optimization

by

John Marc Shewchun

B.A.Sc. Aerospace Engineering

University of Toronto, 1995

Submitted to the Department of Aeronautics and Astronautics
on August 8, 1997, in partial fulfillment of the
requirements for the degree of
Master of Science in Aeronautics and Astronautics

Abstract

Constrained control problems are ubiquitous. Since we cannot escape them, the only alternative is to develop "sound" methodologies for dealing with them. That is, we must provide methods that have specific guarantees as dictated by the problem, otherwise we cannot say with certainty that our control decision will result in a stable or safe system. In particular, two different, but related, constrained control areas are investigated. The first is the problem of Linear Time Invariant systems subject to nonlinear actuators. That is, actuators that have symmetric or asymmetric position constraints and possibly rate constraints. The second problem is the detection and resolution of aircraft conflicts. Both problems are very pressing in their own distinct ways. For the first problem a nonlinear state feedback methodology is developed that has guaranteed constraint satisfaction and global asymptotic stability. This is brought about by scheduling the gain to avoid saturation at all times, and is accomplished through a set of nested invariant ellipsoids that for each gain approximate the maximal invariant set. A comparison to sub-controllable sets and an application to the F/A-18 are given. The second problem is approached through a two phase method. Firstly, aircraft conflicts are detected by performing a worst case analysis of the situation through Linear Matrix Inequality feasibility problems. Once this is completed the resolution problem is approached by formulation as a convex optimization problem. The resulting strategy is highly combinatorial in its complexity. A possible solution to this problem is attempted by formulation of a lower bound obtained by convex optimization techniques.

Thesis Supervisor: Eric Feron
Title: Assistant Professor

Acknowledgments

First and foremost I would like to thank Eric Feron for the opportunity to come to MIT and work on a very challenging research topic. Without his guidance this thesis would not have been possible.

Thank you to all of the members of the Instrumentation, Control, and Estimation group, both past and present. Your helpful discussions and most importantly your friendship made my stay an enjoyable one.

Contents

1	Introduction	15
1.1	Background and Previous Results	18
1.1.1	Linear Systems with Pointwise-in-Time Constraints	19
1.1.2	Conflict Detection and Resolution	21
1.2	Outline	21
2	Preliminaries and Problem Statement	23
2.1	Convex Optimization and LMIs	23
2.1.1	Schur Complements	25
2.1.2	Duality and the Quadratically Constrained Quadratic Program	25
2.2	Lyapunov Stability Theory and Invariant Sets	28
2.3	Constrained Control Problems	31
2.3.1	Asymptotic null controllability with bounded controls	33
3	Nonlinear State Feedback for Constrained Control	35
3.1	Position Constraints	38
3.1.1	An Academic Example	44
3.1.2	Limit Properties of Invariant Ellipsoids	46
3.2	Asymmetric Controls	49
3.2.1	Example of Asymmetric Control	54
3.3	Position and Rate Constraints	57
3.3.1	LQR Based Solution	57
3.3.2	Performance Enhancements via LMIs	66

3.4	Comparison with Reachable Sets	70
3.4.1	Sub-Reachable Sets	70
3.4.2	Extension to Controllable Sets with State Constraints	74
3.5	Application to the F/A-18 HARV	77
3.5.1	Controller Design	79
4	Conflict Detection and Resolution	83
4.1	Conflict Detection	84
4.2	3-Dimensional Case	93
4.3	Conflict Resolution	97
4.4	Computation of the Lower Bound	102
5	Conclusions and Recommendations	109
5.1	Nonlinear Control for Nonlinear Actuators	109
5.2	Convex Optimization for Aircraft Conflict Detection and Resolution .	111

List of Figures

1-1	Nonlinear Actuator Model	16
3-1	The Sets \mathcal{L} , \mathcal{M} , and \mathcal{N}	36
3-2	Nested Ellipsoids	42
3-3	Nested Ellipsoids for Double Integrator	45
3-4	States and Control for Double Integrator	45
3-5	Open Loop Unstable System	47
3-6	Asymmetric Ellipsoids for Spring Mass System	54
3-7	States and Control for Spring Mass System: Example 1	56
3-8	States and Control for Spring Mass System: Example 2	56
3-9	Invariant Ellipsoid Set for Single Integrator	65
3-10	Performance of Single State System	66
3-11	LMI Invariant Ellipsoid Set for Single Integrator	70
3-12	Performance of Single State system with LMI Enhancements	71
3-13	Sub-Controllable Set for Double Integrator	74
3-14	Performance for Sub-Controllable Set Controller	75
3-15	Sub-Controllable Set for State Constrained System	77
3-16	Performance for Sub-Controllable State Constrained Controller	78
3-17	F/A-18 HARV Nonlinear Model	78
3-18	Single Side Turn Response	82
3-19	Control Surface Positions and Rates	82
4-1	Uncertainties in the Velocities	85
4-2	Uncertain Switch Time	89

4-3	Uncertain Acceleration	91
4-4	3-Dimensional Case	93
4-5	Relative Motion and Admissible Regions	99
4-6	Constraints on Aircraft Velocities	101
4-7	Frequency of Null Eigenvector	106
4-8	Example of a 4 Aircraft Conflict	107
4-9	Null Space Parameterization	108

List of Tables

3.1	3% Settling Times for Asymmetric Control Examples	55
3.2	Performance for F/A-18 HARV Example	81
4.1	Null Eigenvector Solution Percentages	107

Notation

$\mathbf{R}, \mathbf{R}^k, \mathbf{R}^{m \times n}$ The real numbers, real k -vectors, real $m \times n$ matrices.

\mathbf{R}_+ The nonnegative real numbers.

$\bar{\mathbf{R}}_+$ The positive real numbers.

\mathbf{I}_+ The nonnegative integers.

I_k The $k \times k$ identity matrix.

M^T Transpose of a matrix $M : (M^T)_{ij} = M_{ji}$.

$\text{Tr}M$ Trace of $M \in \mathbf{R}^{n \times n}$, *i.e.*, $\sum_{i=1}^n M_{ii}$.

$M \geq 0$ M is symmetric and positive semidefinite, *i.e.*, $M = M^T$ and $z^T M z \geq 0$ for all $z \in \mathbf{R}^n$.

$M > 0$ M is symmetric and positive definite, *i.e.*, $M = M^T$ and $z^T M z > 0$ for all nonzero $z \in \mathbf{R}^n$.

$M > N$ M and N are symmetric and $M - N > 0$.

$M^{1/2}$ For $M > 0$, $M^{1/2}$ is the unique $Z = Z^T$ such that $Z > 0$, $Z^2 = M$.

$\max(M)$ The maximum element of the matrix M .

$\text{diag}(M)$ Square matrix formed from the diagonal elements of M , *i.e.*, $\text{diag}(M)_{ii} = M_{ii}$, and $\text{diag}(M)_{ij} = 0$ for $j \neq i$.

$\mathbf{diag}(\dots)$ Block-diagonal matrix formed from the arguments.

$M(\alpha, \beta)$ The submatrix formed by the elements of the rows indexed by α and the elements of the columns indexed by β . For example,

$$\begin{bmatrix} 1 & 2 & 3 \\ 4 & 5 & 6 \\ 7 & 8 & 9 \end{bmatrix} (\{1, 3\}, \{1, 2, 3\}) = \begin{bmatrix} 1 & 2 & 3 \\ 7 & 8 & 9 \end{bmatrix}.$$

$\mathcal{E}(M, \alpha)$	The ellipsoidal set defined as $\mathcal{E}(M, \alpha) \equiv \{x \in \mathbf{R}^n : x^T M x \leq \alpha\}$.
$\mathcal{E}(M, \alpha, a)$	The ellipsoidal set defined as $\mathcal{E}(M, \alpha, a) \equiv \{x \in \mathbf{R}^n : (x - a)^T M (x - a) \leq \alpha\}$.
$\mathcal{E}^{-1}(M, a)$	The ellipsoidal set defined as $\mathcal{E}^{-1}(M, a) \equiv \{x \in \mathbf{R}^n : (x - a)^T M^{-1} (x - a) \leq 1\}$.
$\mathcal{H}(c)$	The hyperslab defined as $\mathcal{H}(c) \equiv \{x \in \mathbf{R}^n : c^T x \leq 1\}$.
$\mathcal{P}(c)$	The hyperplanes defined as $\mathcal{P}(c) \equiv \{x \in \mathbf{R}^n : c^T x = 1\}$.
$\ \cdot\ $	The standard n -dimensional Euclidean norm, <i>i.e.</i> $\ x\ = \sqrt{x^T x}$.

Chapter 1

Introduction

Constrained control problems are ubiquitous. Whether it is the mechanical limitations of an actuator, or the amount of cash that a company has available for investment in a new venture, the control of any dynamic system will always involve real physical constraints on the states and inputs that must be considered. Sometimes, these constraints may be weak, in that, for all intensive purposes they can be ignored. However, in many cases they are severe and disregarding them in a control decision or design could easily lead to disaster. The point is that since they cannot be avoided, sound methodologies must be developed to deal with them. The point of departure for this thesis will be the constrained control of Linear Time Invariant (LTI) systems. In particular, systems that have nonlinear actuators or systems that have more general state and control constraints.

One of the most typical input constraints for LTI systems results from nonlinear actuators. Indeed, all actuators are nonlinear since they are unable to respond to an input above a certain level. These are hard constraints because the actuator simply does not respond if the constraint is violated. Fig. 1-1 shows a typical model of an actuator that has linear dynamics, position saturation, and rate limiting; which could be used to represent the servo that drives an aircraft control surface. The actual control input u will be a linear function of the commanded input u_c only when u_c is within the saturation and rate limit bounds. However, when the actuator is driven above the saturation or rate limit within a feedback loop the performance can

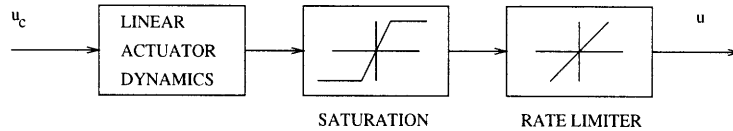


Figure 1-1: Nonlinear Actuator Model

be radically reduced, and the system could possibly be driven unstable. One such problem, that applies to pure saturation only, is known as integrator windup, where an integrator in the control loop builds up to a value greater than the saturation limit of the actuator. When the integrator finally begins to unwind the resulting control signal can become badly out of phase and result in severe oscillations, see pg. 79 in [76] for a brief discussion. It has also been observed that multiple saturations change the direction of the controls resulting in improper plant inversion [35]. Even more recently is the identification that actuator rate saturation poses a severe problem to modern combat aircraft. High performance aircraft are constantly pushing the limits of available performance. The phase lag induced by rate limiting has been shown to produce a significant tendency for Pilot Induced Oscillations (PIOs) [36, 29]. Yet another nonlinear actuator problem occurs when the position saturation limits are non-symmetric. This problem is present in a large number of actuation problems, yet few techniques have been developed that directly take asymmetric constraints into account. In response to these problems a wealth of techniques and methodologies have been put forward, and recently much renewed interest has taken place, see for example the recent journal [4].

Another important problem that can be cast in the constrained control of LTI systems category is aircraft conflict detection and resolution. The definition of an aircraft conflict is quite simple. Given a portion of airspace, a conflict between two aircraft is declared when their predicted positions are such that both a specified horizontal and vertical separation parameter are infringed [30]. The separation parameters rep-

resent a desired safety margin which cannot be violated. Even before the conflict can be resolved it must be detected by analyzing the situation. Once the analysis technique has declared a conflict the resolution problem is to determine trajectories, for all aircraft involved, that will eliminate the threat of a collision. Thus we have a combined detection and resolution problem and the two are inseparable. Although the detection/resolution problem is quite simple in formulation, its solution is extremely difficult due to the combinatorial nature of the problem. For two aircraft the situation is well understood, and analytical detection and resolution methods exist [56, 42]. However, the worst case number of computations needed in the conflict detection problem grows with the square of the number of aircraft [69]. Even more significant, the worst case number of computations in the resolution problem can grow as two to the square of the number of aircraft [18]. Motivation to provide new methodologies for dealing with this situation has been increasing. Most recently, under the concept of Free Flight, rigid airway structures and other constraints on aircraft trajectories will be greatly reduced [3]. Aircraft will be allowed to plan their own trajectories in order to optimize a range of flight variables. The resulting flexibility will require more sophisticated automated conflict detection and resolution. In particular both pilots and ground controllers, with the aid of automated systems, will be responsible for predicting and avoiding collisions. It is easy to see why such a problem is really a constrained control problem. In resolving a conflict there are really only two possibilities. Conflicts can be solved horizontally by issuing each aircraft a turn maneuver, or vertically by specifying climb and descent rates. It must therefore be taken into account that the aircraft have limits on rates of turn and climb [41]. Indeed, this is similar to the nonlinear actuator in that there are hard constraints on aircraft maneuverability. Furthermore, it follows that the condition that any two aircraft not violate a given separation parameter is a state constraint. Underlying this is the absolute necessity for safety. Human lives are at risk, and thus resolution methods must provide guarantees of safety. All of this poses a challenging constrained control problem.

We usually use the term admissible when referring to system states and control

inputs that satisfy the problem statement. Thus the problem of constrained control can be succinctly defined as selecting the best (in some pre-defined sense) possible admissible control such that the state constraints are never violated (*i.e.* the state is always admissible). Clearly, both of the problems described above fall into this description. Furthermore, we are really implicitly describing an optimization problem. The term best implies that we will choose some performance index that is to be maximized. As we will see, one of the difficulties that follows from this is the representation of the admissible sets. Our approach will be one of convex approximation, that is defining all admissible sets in terms of convex ones.

In this thesis we will bring to light two methodologies for solving the constrained control problems described above. The first is a closed loop feedback control for dealing with nonlinear actuators. The second is a more general method for control that is motivated by and presented through the aircraft conflict detection and resolution problem. Underlying the two methods are two crucial goals. First, we desire numerically efficient methods. By numerically efficient we mean that the methods must have guaranteed solution times and are possibly implementable in real time. Secondly, is the desire to provide as many guarantees on the solution in terms of stability and performance (*i.e.* optimality). As stated, one of the tools we will make large use of to aid in this pursuit will be convex optimization. In short, convex optimization is any optimization problem for which the objective and constraints are convex functions. There are many benefits that arise from using convex optimization. An important one is the fact that any locally optimal solution is guaranteed to be globally optimal. Also, convex optimization problems have guaranteed computational solution times [54].

1.1 Background and Previous Results

This section briefly details some of the more important results relating to this thesis. For convenience it will be divided into two groups, the first dealing with LTI systems and nonlinear actuators, and the second dealing with the issue of aircraft conflict

resolution.

1.1.1 Linear Systems with Pointwise-in-Time Constraints

The term "Pointwise-in-Time Constraints" was introduced by E. G. Gilbert at the 1992 American Control Conference [25]. This is not to say that pointwise-in-time constraints are anything new. Indeed, Engineers have long understood that real systems possess many physical constraints. The nonlinear actuator presented above certainly classifies as a pointwise-in-time constraint and represents one of the most actively researched types. In particular, most of the research revolves around the base problem, that is, nonlinear actuators with position constraints only.

Some of the earliest and most practical design methods for nonlinear actuators are the so called 'anti-windup' schemes, where the control input is adjusted, usually by some gain, so that saturation is avoided and performance is improved. This is still a very active area of research, see [6, 40] for example. A large part of the recent work to develop theory and control designs that solve these problems relies on Lyapunov stability theory. This is not without reason. Lyapunov stability theory provides a simple and powerful way to deal with nonlinear systems and forms the basis for much of the research in that field. It has also become extremely useful in linear system theory for the stability and robustness analysis of linear systems in the presence of plant uncertainty and parameter variation. The work of McConley *et. al.* is a good example of some of the recent control synthesis work using control Lyapunov functions to provide robust stability for nonlinear systems [48].

An important theoretical result was the discovery and proof that, in general, global asymptotic stabilization of input constrained systems cannot be achieved by means of saturated linear control laws [21, 72]. These results were then extended to show that global stabilization can be achieved by a combination of nested saturations resulting in a nonlinear feedback law [74, 71]. It is important to note that these results do not preclude the use of saturated linear feedback laws. Indeed, the low-and-high gain controller presented in [61] establishes the notion of semi-global stabilization. That is, the region of stabilization can be made arbitrarily large by reducing the gain of the

controller. This work has been extended to cover several classes of problems, including global stability, as presented in [32]. Implicit and explicit in much of the research on constrained control is the use of positively invariant sets for the synthesis of both linear and nonlinear feedback laws. A saturated linear controller for continuous and discrete time systems was designed using an ellipsoidal approximation of the maximal invariant set in [28]. This work was advanced to discrete time systems with polyhedral control and state constraints where a linear variable structure controller was synthesized [27]. The global stabilization of an n -fold integrator using a saturated linear controller was discussed in [33]. The existence of positively invariant polyhedral sets and linear controllers for discrete and continuous time systems were established in [79, 9]. Based on the existence result, it was then shown that the maximal regions of attraction could be arbitrarily approximated by polyhedral sets [26]. Following the work on computing maximal invariant sets, controllers were designed for continuous time systems [11, 12, 10]. A method for computing a nonlinear state feedback controller based on off-line computation was proposed in [47]. Robust constrained control schemes for the rejection of disturbances have been posed in [73, 49]. A model predictive control that has characteristics similar to the methodology that will be discussed here was presented in [39]. All of these methods, in some way, have a commonality with the approach that will be presented here.

The issue of nonlinear actuators with rate saturation is very recent. Several of the established techniques have been extended to this problem in [43, 45, 44, 46, 34, 62, 8]. Highly practical methods have also been proposed for dealing with rate limiting via software limiters in [31, 60].

Some of the earliest control synthesis work using positively invariant sets was centered around finding a "controllability function" that directly provided a Lyapunov function guaranteeing stability and boundedness of the controls [23, 38]. This work was advanced through the context of reachable and controllable sets to provide further nonlinear control schemes for bounded control and is based on the method of ellipsoids [17, 37, 70]. Indeed, this research is some of the most closely related to what will be presented here.

1.1.2 Conflict Detection and Resolution

Unlike their pointwise-in-time counter parts, algorithms to deal with anti-collision problems for air transportation have been studied with far less of a concern for guarantees on performance and computational running times. An extensive survey of existing conflict detection and resolution methodologies has recently been compiled in [42]. Additionally, the recent report by Krozel, Peters, and Hunter provides an introduction to the problem and presents a detailed analysis of the use of optimal control type problems for conflict resolution [41]. Many authors have brought many tools to bare. In [85] the author uses the concept of symmetrical force fields, developed originally for robots, to present a self-organizing (the aircraft resolve conflicts without any communication or negotiation) conflict resolution methodology. Another self-organizational approach is the 'Pilot Algorithm' presented in [19]. The use of powerful genetic algorithms has been used to address large scale problems with many constraints [18]. Variational calculus techniques have been applied in [67] to sequence aircraft arrivals at airports. Monte-Carlo methods have been used to develop statistical conflict alerting logic for free flight and closely spaced parallel approaches [84, 16]. An innovative approach based on hybrid control systems technology was proposed in [75]. Other interesting attempts at optimal resolution strategies have been researched in [20, 50, 80]. Coupled with this research is the necessity for safety and efficiency in the newly proposed Free Flight environment stated in the RTCA report [3].

1.2 Outline

The outline of this thesis is as follows.

Chapter 2 first presents some background knowledge on Convex Optimization and Lyapunov stability theory that will be needed in this thesis. In addition the four constrained control problems that will be investigated are formulated with some limited discussion.

Chapter 3 presents a nonlinear state feedback control methodology that is used to solve the first three constrained control problems. Several examples are given

to demonstrate the method. The chapter closes with a comparison to the field of reachable sets and with an application of the methodology to a nonlinear simulator of the F/A-18 HARV.

Chapter 4 presents a methodology for aircraft conflict detection and resolution that can be used to solve constrained control problems with quite general state and control constraints.

Finally Chapter 5 presents the conclusions and suggestions for future research.

Chapter 2

Preliminaries and Problem Statement

In this chapter we present some preliminaries needed for the developments that follow along with statements of the problems that will be investigated. Two primary tools will be needed, that of convex optimization and Lyapunov stability. We will present only a brief overview of the properties of each that are important here.

2.1 Convex Optimization and LMIs

Convex optimization is a very general term that applies to optimization problems in the standard form:

$$\begin{aligned} & \text{minimize } f_0(x) \\ & \text{subject to } f_i(x) \leq 0, \quad i = 1, \dots, m, \end{aligned} \tag{2.1}$$

where the objective $f_0(x)$ and the constraints $f_i(x)$ are convex functions (see [58] for a definition of convex functions). The fundamental property of convex optimization is that any locally optimal point is also globally optimal [15]. In other words if we can solve (2.1) then we are guaranteed to obtain the best possible solution. Both linear programming and convex quadratic programming are classes of convex optimization problems. In the development that follows we will be concerned with two important types of convex optimization problems known as semidefinite programming (SDP)

and determinant maximization (MAXDET) problems. The SDP problem is really a subset of the more general MAXDET problem which can be formulated as

$$\begin{aligned} & \text{minimize } c^T x + \log \det G(x)^{-1} \\ & \text{subject to } G(x) > 0, F(x) > 0, \end{aligned} \tag{2.2}$$

where $x \in \mathbf{R}^n$ is the optimization variable. Furthermore, the functions $G : \mathbf{R}^n \rightarrow \mathbf{R}^{l \times l}$, and $F : \mathbf{R}^n \rightarrow \mathbf{R}^{m \times m}$ are defined as

$$\begin{aligned} G(x) &\equiv G_0 + \sum_{i=1}^n x_i G_i \\ F(x) &\equiv F_0 + \sum_{i=1}^m x_i F_i, \end{aligned} \tag{2.3}$$

where $G_i = G_i^T$ and $F_i = F_i^T$ for $i = 1, \dots, m$. Now since the inequality signs in (2.2) denote matrix inequalities, and from (2.3) these inequalities depend affinely on the variable x , we refer to them as Linear Matrix Inequalities (LMIs). If the set of variables x that cause the matrix inequality to be satisfied is non-empty, then a matrix inequality is referred to as *feasible*. We will encounter problems in which the variables are matrices. In this case we will not write out the LMI explicitly in the form $F(x) > 0$, but instead make it clear which matrices are the variables.

When the log function is removed from (2.2) we have the standard form of an SDP:

$$\begin{aligned} & \text{minimize } c^T x \\ & \text{subject to } F(x) > 0. \end{aligned} \tag{2.4}$$

In addition to being convex these problems are solvable in polynomial time. That is, the computational time is proportional to some polynomial that is a function of the number of problem variables and constraints. Of importance is the number of problems that can be cast in this form. The recent book by Boyd *et. al.* presents a detailed list of system and control theory problems that can be formulated as LMIs and solved via SDP and MAXDET problems [14]. In addition, there exist several software packages that solve problems of this type [22, 77, 83].

2.1.1 Schur Complements

One of the more useful properties of LMIs is the ability to also write convex matrix inequalities that are quadratic in a variable as an LMI. These nonlinear, yet convex, inequalities can be converted to LMI form using Schur complements. In particular, a variable x exists such that

$$\begin{bmatrix} Q(x) & S(x) \\ S(x)^T & R(x) \end{bmatrix} > 0, \quad (2.5)$$

if and only if

$$R(x) > 0, \quad Q(x) - S(x)R(x)^{-1}S(x)^T > 0, \quad (2.6)$$

where $Q(x) = Q(x)^T$, $R(x) = R(x)^T$, and $S(x)$ depend affinely on x .

An example is that we will see in the sequel is the constraint $c(x)^T P(x)^{-1} c(x) < 1, P(x) > 0$, where $c(x) \in \mathbf{R}^n$ and $P(x) = P(x)^T \in \mathbf{R}^{n \times n}$. This constraint is useful for representing geometric constraints on the matrix P , and can be expressed as the LMI

$$\begin{bmatrix} P(x) & c(x) \\ c(x)^T & 1 \end{bmatrix} > 0. \quad (2.7)$$

2.1.2 Duality and the Quadratically Constrained Quadratic Program

An important concept in convex optimization is that of duality. The basic idea is to take into account the constraints in (2.1) by augmenting the objective function with a weighted sum of the constraint functions. To this end we define the Lagrangian as

$$L(x, \lambda) = f_0(x) + \sum_{i=1}^m \lambda_i f_i(x), \quad (2.8)$$

where $\lambda_i \geq 0$, $i = 1, \dots, m$, is the Lagrange multiplier or dual variable associated with the constraint $f_i(x) \leq 0$. For $\lambda \in \mathbf{R}^m$ the dual function $g(\lambda)$ is the minimum

value of the Lagrangian over x and can be written as

$$g(\lambda) = \inf_x L(x, \lambda) = \inf_x \left(f_0(x) + \sum_{i=1}^m \lambda_i f_i(x) \right). \quad (2.9)$$

Note that this is now an unconstrained minimization problem and we say that λ is *dual feasible* if $g(\lambda) > -\infty$. The important property of the dual function (2.9) is that it provides a lower bound on the solution to the convex optimization problem (2.1). That is, given that p^* is the optimal value of the problem (2.1) we have

$$g(\lambda) \leq p^* \quad (2.10)$$

for any $\lambda \geq 0$ [15]. Naturally we are left with the question, what is the best possible lower bound we can obtain? This can be answered by solving the convex optimization problem

$$\begin{aligned} & \text{maximize } g(\lambda) \\ & \text{subject to } \lambda \geq 0. \end{aligned} \quad (2.11)$$

This problem is usually referred to as the dual problem associated with the primal problem (2.1). Also note that the dual problem is convex even when the primal problem is not. This is due to the fact that $g(\lambda)$ is always concave. Let the optimal value of the dual problem be denoted by d^* . We already know that

$$d^* \leq p^*.$$

This property is called *weak* duality. Under certain conditions it is possible to obtain *strong* duality in that

$$d^* = p^*.$$

There are many results that establish conditions on f_0, \dots, f_m under which strong duality holds. One of these is known as Slater's condition which asserts that strong duality holds if the problem (2.1) is strictly feasible, *i.e.* there exists an x such that $f_i(x) < 0$, $i = 1, \dots, m$. [15].

The Quadratically Constrained Quadratic Program

In particular we will require the use of the nonconvex Quadratically Constrained Quadratic Program (QCQP):

$$\begin{aligned} & \text{minimize } x^T P_0 x + 2q_0^T x + r_0 \\ & \text{subject to } x^T P_i x + 2q_i^T x + r_i \leq 0, \quad i = 1, \dots, n, \end{aligned} \tag{2.12}$$

where $P_i = P_i^T$. Thus we are considering a possibly nonconvex problem because the P_i are indefinite. In an equivalent derivation to that above we can form the Lagrangian via a method that is known as the \mathcal{S} -procedure [14]. This gives

$$\begin{aligned} L(x, \lambda) &= x^T P_0 x + 2q_0^T x + r_0 + \sum_{i=1}^n \lambda_i (x^T P_i x + 2q_i^T x + r_i) \\ &= x^T P(\lambda) x + 2q(\lambda)^T x + r(\lambda), \end{aligned} \tag{2.13}$$

where,

$$\begin{aligned} P(\lambda) &= P_0 + \lambda_1 P_1 + \dots + \lambda_n P_n \\ q(\lambda) &= q_0 + \lambda_1 q_1 + \dots + \lambda_n q_n \\ r(\lambda) &= r_0 + \lambda_1 r_1 + \dots + \lambda_n r_n. \end{aligned} \tag{2.14}$$

From this we obtain the dual function

$$g(\lambda) = \inf_x L(x, \lambda) = \begin{cases} -q(\lambda)^T P(\lambda)^\dagger q(\lambda) + r(\lambda) & \text{if } P(\lambda) \geq 0 \\ -\infty & \text{otherwise,} \end{cases} \tag{2.15}$$

where $(\cdot)^\dagger$ is the pseudo-inverse defined by

$$(I - P(\lambda)P(\lambda)^\dagger)q(\lambda) = 0.$$

We know that the function $g(\lambda)$ has the property that for any given λ its value is less than or equal to the optimal value of the QCQP. Thus, a lower bound for the QCQP

can be found by solving the dual problem ([78]):

$$\begin{aligned} & \text{maximize} && -q(\lambda)^T P(\lambda)^\dagger q(\lambda) + r(\lambda) \\ & \text{subject to} && \lambda \geq 0. \end{aligned} \tag{2.16}$$

Slater's condition, described above, states that if the objective and constraints are strictly convex then strong duality holds. In the nonconvex case there are still cases where strong duality holds. For example, if there is only one constraint, or if there are two constraints and x is a complex variable [14].

By the use of Schur complements we can convert the QCQP dual problem into the LMI formulation:

$$\begin{aligned} & \text{maximize} && \gamma \\ & \text{subject to} && \begin{bmatrix} -P(\lambda) & q(\lambda) \\ q(\lambda)^T & \gamma - r(\lambda) \end{bmatrix} \leq 0 \\ & && \lambda \geq 0. \end{aligned} \tag{2.17}$$

Note that this removes the pseudo inverse of $P(\lambda)$. We will use this particular formulation in Chapter 4 to obtain a lower bound on the aircraft conflict resolution problem.

2.2 Lyapunov Stability Theory and Invariant Sets

In addition to the tools of convex optimization we will also need to use some of the basic results from the well known field of Lyapunov stability theory. We will not provide proofs for any of the theorems in this section since they can all be obtained from [68] or many other books on linear and nonlinear systems. In order to determine if a system is stable we must first define what stability is. The classic definition of Lyapunov stability is well known and defined as follows.

Definition 2.1 ([68]) *The equilibrium state $x = 0$ is said to be stable if, for any $R > 0$, there exists $r > 0$, such that if $\|x(0)\| < r$, then $\|x(t)\| < R$ for all $t \geq 0$.*

Often though this definition of stability is not strong enough, since it does not imply that the state converges to the origin. Thus we provide the stronger notion of asymptotic stability.

Definition 2.2 ([68]) *An equilibrium point 0 is asymptotically stable if it is stable, and if in addition there exists some $r > 0$ such that $\|x(0)\| < r$ implies that $x(t) \rightarrow 0$ as $t \rightarrow \infty$.*

If either of these notions holds for any initial condition then the system is said to be globally stable or globally asymptotically stable.

Most of the power of Lyapunov stability theory revolves around what is often called Lyapunov's Direct Method. Essentially it consists of finding an energy function that can be used to determine the stability of the system. Using such a function the global asymptotic stability can be formulated in the following theorem.

Theorem 2.1 ([68]) *Assume that there exists a scalar function V of the state x , with continuous first order derivatives such that*

- $V(x)$ is positive definite
- $\dot{V}(x)$ is negative definite
- $V(x) \rightarrow 0$ as $\|x\| \rightarrow 0$

then the equilibrium at the origin is globally asymptotically stable.

The function $V(x)$ is referred to as a Lyapunov function if it satisfies the conditions of Theorem 2.1. Lyapunov functions play an essential role in the analysis of nonlinear systems.

Another powerful notion of stability that follows from these definitions is the concept of invariant sets.

Definition 2.3 ([68]) *A non-empty subset Ω of \mathbf{R}^n is invariant for a dynamic system if every trajectory which starts from a point in Ω stays in Ω for all future time.*

The notion of invariant sets is useful in many applications not the least of which is constrained control. It is easy to see that a bounded invariant set places limits on the state of the system. Thus if we know the relation between the admissible controls and the corresponding invariant sets it is possible to provide a guaranteed solution to the constrained control problem. Much of the effort evolves around computing these invariant sets given certain constraints on the input. A very useful theorem in this endeavor is based on linear systems. First, consider the Linear Time Invariant (LTI) system in the standard form

$$\dot{x} = Ax + Bu, \quad x(0) = x_0, \quad (2.18)$$

where $x \in \mathbf{R}^n$ is the state and $u \in \mathbf{R}^m$ is the control input.

Theorem 2.2 (Adapted from [68]) *The system (2.18) with state feedback, $u = Kx$, is asymptotically stable if and only if there exists a symmetric positive definite matrix P such that*

$$(A + BK)^T P + P(A + BK) < 0. \quad (2.19)$$

Equivalently by multiplying either side by $P^{-1} = \Gamma$

$$\Gamma(A + BK)^T + (A + BK)\Gamma < 0. \quad (2.20)$$

Furthermore, the sets, $\mathcal{E}(P, \alpha), \mathcal{E}^{-1}(\Gamma, \alpha)$ are invariant under the control u for any $\alpha \in \mathbf{R}_+$.

Essentially this theorem says that asymptotic stability of the system (2.18) under a state feedback control is equivalent to the existence of a matrix P that satisfies (2.19). Clearly, the sufficiency follows from using $V = x^T P x$ as a Lyapunov function for the closed loop system. Also, note that the conditions (2.19,2.20) are LMIs in the variables P and Γ .

2.3 Constrained Control Problems

In this section we present the constrained control problems that will be solved in the following development. Throughout what follows we will be considering the LTI system (2.18). The first problem represents the system (2.18) subject only to position saturation. This forms the fundamental, or base, problem around which a considerable amount of research has been performed. The approach given here will be to find a nonlinear state feedback that globally asymptotically stabilizes the system.

Problem 1 *Nonlinear State Feedback with Position Limits (NSFP)*

Consider the system (2.18) with the position constraints

$$|u_i| \leq \bar{u}_i, \quad i = 1, \dots, m. \quad (2.21)$$

Compute a nonlinear control law, $u = K(x)x$, such that the equilibrium ($x = 0$) of the closed-loop system in the presence of (2.21) is globally asymptotically stable.

Note that the u_i are not necessarily equal. However, it is always possible to normalize these values to unity by defining

$$C_s = \mathbf{diag}(\bar{u}_1, \dots, \bar{u}_m),$$

and using the input substitution,

$$\bar{B} = BC_s.$$

This does not mean that we are ignoring the possibility of a system, such as an aircraft, that has multiple actuators with multiple bounds. We have simply transferred the information into the B matrix and we will see in the next chapter how the possibly unequal values of the \bar{u}_i are taken into account.

Problem 2 *Nonlinear State Feedback with Asymmetric Position Limits (NSFAP)*
 Consider the system (2.18) with the position constraints

$$\underline{u}_i \leq u_i \leq \bar{u}_i, \quad i = 1, \dots, m. \quad (2.22)$$

Compute a nonlinear control law, $u = K(x)x + u_f$, such that the equilibrium of the closed-loop system in the presence of (2.22) is globally asymptotically stable.

Asymmetric control problems such as this usually arise from two possible situations. The first is an asymmetric actuator that does not provide the same control power in both directions. The second is the desire to regulate about some non-zero set point that requires a non-zero control input. In essence these problems are equivalent and one can be converted into the other. For example, consider the problem of regulating about some reference state x^* . Obviously for this to be possible there must exist a u^* such that

$$Ax^* + Bu^* = 0.$$

The addition of u^* to u transforms the symmetric controls (2.21) into the asymmetric controls (2.22). We will use such an interpretation in the reverse direction to solve the NSFAP problem. That is, in solving the NSFAP problem we will use the knowledge that an asymmetric control can imply a reference state.

As with the NSFP problem we can always normalize the constraints such that $\bar{u}_i - \underline{u}_i = 2$ by defining

$$C_a = \mathbf{diag}((\bar{u}_i - \underline{u}_i)/2, \dots, (\bar{u}_i - \underline{u}_i)/2),$$

and using the input substitution,

$$\bar{B} = BC_a.$$

In the last of the nonlinear actuator problems we have the addition of actuator rate constraints, but without any asymmetry.

Problem 3 *Nonlinear State Feedback with Position and Rate Limits (NSFPR)*

Consider the system (2.18) with the position and rate constraints

$$\begin{aligned} |u_i| &\leq \bar{u}_i, \\ |\dot{u}_i| &\leq \bar{\dot{u}}_i, \quad i = 1, \dots, m. \end{aligned} \tag{2.23}$$

Compute a nonlinear control law, $u = K(x)x$, such that the equilibrium of the closed-loop system in the presence of (2.23) is globally asymptotically stable.

Finally, we have the fourth problem motivated by the aircraft conflict detection and resolution problem.

Problem 4 *Control Decisions in the presence of General Constraints (CDGC)*

Consider the system (2.18) subject to the state and control constraints

$$x(t) \in \Omega_s, \quad u \in \Omega_c, \tag{2.24}$$

where Ω_s and Ω_c are given sets. Compute the command u such that the constraints (2.24) are satisfied.

This composes by far the most general of the four problems. In fact, it may not always be possible to solve this problem, nor will we attempt to exactly solve it. However, we will present a methodology for dealing with problems of this type through the example of aircraft conflict detection and resolution.

2.3.1 Asymptotic null controllability with bounded controls

As with normal linear system theory we need to define a notion of controllability for systems with bounded inputs. In the literature this is known as asymptotic null controllability with bounded controls.

Definition 2.4 ([71]) *The system (2.18) is asymptotically null controllable with bounded controls (ANCBC) if for every $x \in \mathbf{R}^n$ there exists an open-loop control that steers x to the origin in the limit as $t \rightarrow \infty$ and satisfies $|u(t)| \leq 1$ for all t .*

It has been shown in [64] that the ANCBC property is equivalent to the algebraic conditions.

1. $[A, B]$ is stabilizable.
2. all eigenvalues of A are located in the closed left half plane.

For the nonlinear actuator problems this will be the standard assumption.

Assumption 2.1 ([44, 64]) *The open loop system is asymptotically null controllable with bounded controls.*

Essentially, Assumption 2.1 will allow us to achieve global asymptotic stability. The problem for unstable systems is that for large initial conditions it often requires a large amount of control to stabilize the system, thus global stability with a bounded control is not possible. For critically stable systems only an infinitesimal control, in principle, is needed to stabilize the system.

In order to ensure that the solution to the Linear Quadratic Regulator problem is positive definite we will require the following.

Assumption 2.2 *The pair $[A, Q^{1/2}]$ is observable, where $Q = Q^T \geq 0$.*

Using these assumptions we are now ready to solve the first three constrained control problems.

Chapter 3

Nonlinear State Feedback for Constrained Control

In this chapter we present a methodology that can be used to solve Problems 1 to 3. First, consider the simple linear state feedback control $u = Kx$. The set of all initial conditions that do not violate the normalized control constraints (2.21) is

$$\mathcal{L}(K) = \bigcap_{i \in \{1, \dots, m\}} \mathcal{H}(k_i^T), \quad (3.1)$$

where k_i is the i th row of the gain matrix K (\mathcal{H} is the hyperslab defined in the notation) [28]. Associated with $\mathcal{L}(K)$ is the largest invariant set contained in $\mathcal{L}(K)$ given by

$$\mathcal{M}(K) = \bigcap_{t \in [0, \infty)} \left((e^{(A+BK)t})^{-1} \mathcal{L}(K) \right). \quad (3.2)$$

However, $\mathcal{M}(K)$ is not easy to deal with since it can be hard to compute and difficult to represent. Fortunately, the knowledge of Theorem 2.19 provides us with an immediate approximation. In other words, if we can compute a matrix P that satisfies the Lyapunov inequality (2.19) the best the best possible approximation is the set

$$\mathcal{N} = \mathcal{E}(P, \alpha),$$

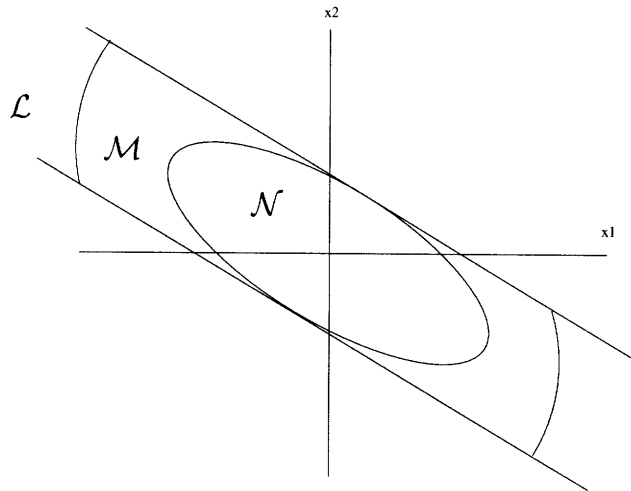


Figure 3-1: The Sets \mathcal{L} , \mathcal{M} , and \mathcal{N}

where $\alpha = 1/\max(\text{diag}(KP^{-1}K^T))$ is found by solving a simple optimization problem. The sets $\mathcal{L}(K)$, $\mathcal{M}(K)$, and \mathcal{N} are shown schematically in Fig. 3-1 for a second order system.

We can now use this knowledge to build a globally stabilizing bounded control. The basic idea is quite straight forward. It is to use low gains, corresponding to a large $\mathcal{M}(K)$, when far from the equilibrium to avoid control saturation, and progressively higher gains, corresponding to a smaller and smaller $\mathcal{M}(K)$, as the state becomes closer to the equilibrium. This idea follows quite intuitively from noting that the control u is a gain-state product Kx . For each K we can use an invariant ellipsoidal approximation to the region $\mathcal{M}(K)$ to guarantee stability and control boundedness. In other words the gain is scheduled to avoid saturation at all times. The challenge arises in finding a computationally efficient manner in which to compute K and P for the best possible performance. The method of choice in this exposition is the Linear Quadratic Regulator (LQR). There are numerous reasons for this choice.

- Solution is optimal with respect to a meaningful quadratic cost.
- Multiloop control design.
- Computationally very cheap (Indeed, it is a convex optimization problem).

- Excellent gain and phase margins.
- Production of a natural Lyapunov function.

The standard LQR problem is to minimize the quadratic performance index

$$J = \int_0^{\infty} (x^T Q x + u^T R u) dt. \quad (3.3)$$

The solution to this problem is found in the matrix P of the Algebraic Riccati Equation (ARE)

$$A^T P + P A - P B R^{-1} B^T P + Q = 0, \quad (3.4)$$

and the associated gain matrix, $K = -R^{-1} B^T P$. The properties of the solution matrix P depend, in general, on the assumptions made about the dynamic system involved. We will be interested in the case where the system is ANCBC, and the properties of the Riccati equation are yielded by the following lemma.

Lemma 3.1 *Let Assumptions 2.1 and 2.2 hold. Take $R = rI_m$, where $r \in \bar{\mathbf{R}}_+$. Then there exists a unique positive definite solution $P(r)$ to the ARE with the following properties*

1. *The matrix $A + BK$ is stable or Hurwitz.*
2. *$P(r)$ is continuously differentiable with respect to r and*

$$\frac{dP(r)}{dr} > 0, \text{ for any } r.$$

3. $\lim_{r \rightarrow 0} P(r) = 0$.
4. *$P(r)$ is an analytic function of r .*
5. *The function $V = x^T P(r)x$, for any r , is a Lyapunov function for the system (2.18) with state feedback $u = Kx$.*

Proof: The proof of items 1-3 follows directly from Lemma 3.1 and Remark 3.2 in [32]. The proof of item 4 is from Theorem 4.1 in [57]. Finally, by direct

computation the function $V = x^T P(r)x$ satisfies the conditions of Theorem 2.1 for any r . ■

3.1 Position Constraints

The methodology presented in the previous section can be used to solve the NSFP problem by means of the following theorem. An almost identical result was first proven by Wredenhagen and Bélanger [81]. The result presented here was first reported in [53].

Theorem 3.1 *Let Assumptions 2.1 and 2.2 hold. Take $R = rI_m$, where $r \in \bar{\mathbf{R}}_+$. Then the control*

$$u = -\frac{B^T P(r)}{r}x,$$

with $P(r)$ the solution to (3.4), and for any time t

$$r(x(t)) = \min r : x(t) \in \mathcal{E}(P(r), \alpha(r)),$$

where

$$\begin{aligned} \alpha(r) &= 1/\max(\text{diag}(K(r)P^{-1}(r)K^T(r))) \\ &= 1/\max(\text{diag}(B^T P(r)B/r^2)), \end{aligned} \tag{3.5}$$

solves Problem 1.

In order to simplify the proof we need to establish some important properties of $\alpha(r)$ that have not been discussed previously. First note that $\alpha(r)$ can also be written as

$$\alpha(r) = 1/\max_{i=1,\dots,m} (b_i^T P(r)b_i/r^2), \tag{3.6}$$

where b_i is the i th column of the B matrix.

Lemma 3.2 *$\alpha(r)$ is a continuous function of r . Furthermore, let i^* be the column number that achieves the maximum in (3.6) (note that it need not be unique). Then either the maximum is achieved by one value of i^* , for all r , or the value of i^* changes only a finite number of times.*

Proof: The proof is in two parts.

a) *α is continuous:* First note that $P(r)$ is a continuous and unique function of r from Lemma 3.1. Then $\alpha(r)$ is continuous by virtue of the fact that the maximum function is continuous and a composition of continuous functions is continuous [59].

b) *finite switchings:* Let r take values on the nonempty bounded interval $[r_1 \ r_2]$, where $r_2 > r_1 > 0$. Consider two columns of the B matrix, b_i and b_j . Assume that $b_i^T P(r) b_i = b_j^T P(r) b_j$ for an infinite number of values of $r \in [r_1 \ r_2]$. Thus by the Bolzano-Weierstrass theorem there exists a limit point r^* . Now, because $P(r)$ is an analytic function of r from Lemma 3.1, Theorem 10.8 in [66] tells us that $b_i^T P(r) b_i = b_j^T P(r) b_j$ over the whole interval $r \in [r_1 \ r_2]$. Thus if i^* switches between two values an infinite number of times the maximum is achieved by both b_i and b_j over the whole interval of r . This can be extended to any arbitrarily large nonempty bounded interval of r and any number of possible maximizers.

Clearly, the only other possibility is that the value of i^* switches only a finite number of times, and thus the lemma is proven. ■

We are now ready to prove Theorem 3.1.

Proof: [Theorem 3.1] The proof consists of three parts. Showing that there exists an invariant ellipsoid for each value of r , that these ellipsoids are nested, and that the outer ellipsoid can be made arbitrarily large.

a) *Invariance:* From item 5 of Lemma 3.1 we have that $V = x^T P(r) x$ is a Lyapunov function for any r . Clearly, we can use Theorem 2.2 to show that the ellipsoid $\mathcal{E}(P(r), \alpha(r))$ is invariant and any trajectory that starts there will not violate the constraints because of the scaling (3.5).

b) *Nesting:* A necessary and sufficient condition for nesting is ([81, 53])

$$\frac{d\tilde{P}(r)}{dr} \leq 0, \tag{3.7}$$

where

$$\tilde{P}(r) = \frac{P(r)}{\alpha(r)}. \tag{3.8}$$

Taking the derivative of (3.4) with respect to r and collecting terms gives

$$A_{cl}^T dP + dP A_{cl} + \frac{PBB^T P}{r^2} dr = 0, \quad (3.9)$$

where $A_{cl} = A - \frac{BB^T P(r)}{r}$. Now consider the case where there is one maximizer \tilde{b} of the function (3.6). Taking the derivative of $\tilde{P}(r)$ with respect to r yields

$$d\tilde{P}(r) = (\tilde{b}^T P \tilde{b}) \frac{dP}{r^2} + \frac{\tilde{b}^T dP \tilde{b} P}{r^2} - 2(\tilde{b}^T P \tilde{b}) \frac{P}{r^3} dr. \quad (3.10)$$

From (3.9) we can write

$$\frac{dP(r)}{dr} = \int_0^\infty e^{A_{cl}^T \tau} \frac{PBB^T P}{r^2} e^{A_{cl} \tau} d\tau, \quad (3.11)$$

and from (3.4) P satisfies

$$P(r) = \int_0^\infty e^{A_{cl}^T \tau} \left(\frac{PBB^T P}{r} + Q \right) e^{A_{cl} \tau} d\tau. \quad (3.12)$$

Substituting (3.11) and (3.12) into (3.10) we eventually obtain (after some manipulation)

$$d\tilde{P}(r) = - \left[\int_0^\infty e^{A_{cl}^T \tau} Q e^{A_{cl} \tau} d\tau \frac{\tilde{b}^T P \tilde{b}}{r^3} + \tilde{b}^T \int_0^\infty e^{A_{cl}^T \tau} Q e^{A_{cl} \tau} d\tau \tilde{b} \frac{P}{r^3} \right] dr. \quad (3.13)$$

Thus the condition (3.7) is satisfied for the case of one maximizer \tilde{b} . Now, $\tilde{P}(r)$ is a continuous function of r , that has a decreasing derivative over a finite number of intervals of r from Lemma 3.2. Thus $\tilde{P}(r)$ is a decreasing function of r over any interval

c) *Global Stability*: Under Assumption 2.1 it clearly takes only an infinitesimally small gain to asymptotically stabilize the system. Thus the gain vector $K(r)$ can be made arbitrarily small and global stability can always be guaranteed [81].

Thus for any value of x_0 there exists a bounded control via the value of r defined by the ellipsoid $\mathcal{E}(P(r), \alpha(r))$ such that the trajectory will always move in towards the

next inner ellipsoid. Furthermore, it is important to note that although the function $V = x^T P(r)x$ is a quadratic Lyapunov function for each particular value of r , the function $V(r) = x^T P(r)x$ over all r is a non-quadratic Lyapunov function. Indeed, the function $V(r)$ can be used to establish global asymptotic stability. ■

This result deserves several comments. For each value of r we arrive at a matrix $P(r)$, and thus a gain $K(r)$. The scaling (3.5) provides us with the best ellipsoidal approximation to the region $\mathcal{M}(K)$, in terms of $P(r)$. The proof of stability in Theorem 3.1 hinges on showing that the set of ellipsoids

$$\Omega = \{\mathcal{E}(P(r), \alpha(r)) : r \in \bar{\mathbf{R}}_+\} \quad (3.14)$$

is nested, *i.e.*,

$$\mathcal{E}(P(r_1), \alpha(r_1)) \subseteq \mathcal{E}(P(r_2), \alpha(r_2)) \text{ for any } r_1 < r_2.$$

Indeed, this is brought about by scaling (3.5). This nesting property binds the construction together. Each ellipsoid defines an invariant region under which the controls are guaranteed not to saturate. Furthermore, the system state will always move towards the next inner ellipsoid guaranteeing a stable system and allowing the controller gain to be steadily increased to improve performance. A schematic of this is shown in Fig. 3-2.

Although this construction is continuous in the parameter r , in practice, only a finite number of ellipsoids are used. The most straightforward and efficient way to do this is to choose a geometric sequence

$$\mathcal{R} = \{r \in \bar{\mathbf{R}}_+ : r = r_{\max}/\lambda^i, i \in \{0, \dots, N\}\}, \quad (3.15)$$

where $r_{\max} \in \bar{\mathbf{R}}_+, N \in \mathbf{I}_+, (\lambda - 1) \in \bar{\mathbf{R}}_+$. The value of r_{\max} must be chosen such that all expected initial conditions will be in the set Ω generated by \mathcal{R} . The other two parameters N and λ can be chosen, as desired, to obtain an even distribution of

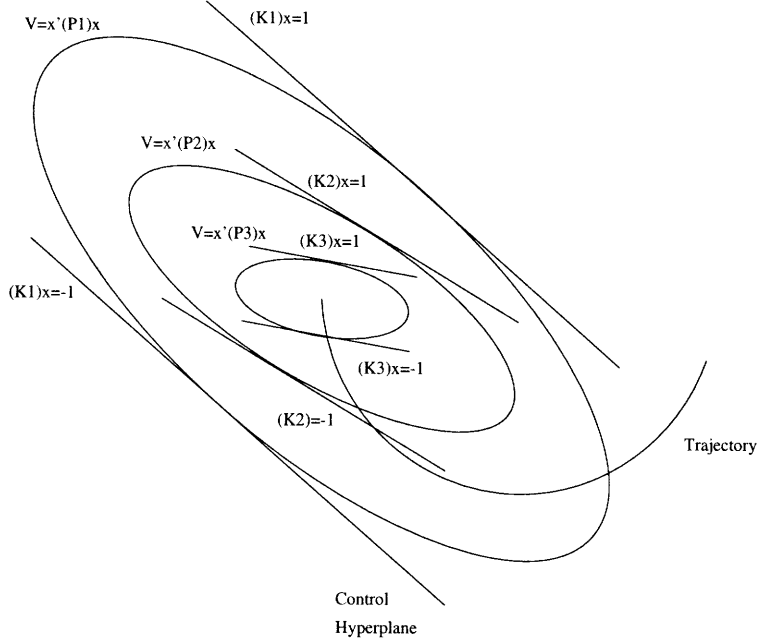


Figure 3-2: Nested Ellipsoids

ellipsoids.

Also, note that the control constraints (2.21) have been normalized to unity as discussed in Section 2.3. This is the most significant difference between the construction of Theorem 3.1 and the results in [81]. The Piecewise-linear Linear Quadratic (PLC) control law developed in [81] uses an iteration function to adjust the elements of the R matrix so that tangency between each ellipsoid and the control planes $\mathcal{P}(k_i^T(r))$ is guaranteed. By tangency we mean that the set $\mathcal{P}(k_i^T(r)) \cap \mathcal{E}(P(r), \alpha(r))$ is non-empty for any r and i .

Instead of choosing the values for r , the PLC law is constructed by choosing values of the parameter ρ for $\mathcal{E}(P, \rho)$. The control weighting matrix is chosen as $R = \text{diag}(\bar{\epsilon}) = \text{diag}(\epsilon_1, \dots, \epsilon_2)$, $\epsilon_i > 0$. Then for a given ρ , $\bar{\epsilon}$ is chosen such that

$$|u_i| = \left| \frac{1}{\epsilon_i} b_i^T P x \right| \leq \bar{u}_i,$$

where b_i is the i th column of the B matrix. It is shown in [81] that for any initial value of $\bar{\epsilon}$ the iteration function

$$\bar{\epsilon}_{n+1} = \sqrt{\rho}\Phi(\bar{\epsilon}),$$

where

$$\Phi(\bar{\epsilon}) = [\phi_1(\bar{\epsilon}), \dots, \phi_m(\bar{\epsilon})]^T,$$

and

$$\phi_i(\bar{\epsilon}) = \frac{1}{\bar{u}_i} \sqrt{b_i^T P b_i},$$

converges to a unique value. An initial value ρ_0 is selected to contain the initial conditions and successive ellipsoids are generated by a reduction factor $\Delta\rho$. However, this does result in an added computational burden because for each ellipsoid in the set a series of iterations must be performed. A simple yet effective way around all of this is to use the gain margin of the LQR ([63]) to guarantee tangency. In particular each gain vector can be scaled as

$$\tilde{k}_i(r) = \frac{k_i(r)}{\sqrt{\alpha(r)k_i(r)P^{-1}(r)k_i^T(r)}}$$

if

$$\tilde{k}_i(r) > \frac{1}{2}k_i(r)$$

which is the gain margin of the LQR. Indeed, this is always the case since the control gains are always increased by this scaling. In a number of simulations this construction always resulted in nearly identical overall performance to the iteration function method. For example, a comparison was performed between the PLC and the High Performance Bounded (HPB) method presented here for the PUMA 560 Robot example given in [81]. In that example the authors use the state energy

$$J = \int_0^\infty x^T Q x dt$$

as a performance measure. With the PLC simulation parameters

$$N = 100, \rho_0 = 1043, \Delta\rho = .94$$

the control law achieved a value of $J_{PLC} = 324$. A controller was constructed for this example using the method described here with the parameters

$$N = 100, r_{\max} = 9000, \lambda = 1.05.$$

The state energy was calculated as $J_{HPB} = 334$ indicating a difference of approximately 3%.

3.1.1 An Academic Example

In this section we will present a simple example that illustrates the High Performance Bounded (HPB) method described above. Consider the double integrator system

$$A = \begin{bmatrix} 0 & 1 \\ 0 & 0 \end{bmatrix} \quad B = \begin{bmatrix} 0 \\ 1 \end{bmatrix}. \quad (3.16)$$

The control law construction parameters in (3.15) were chosen as

$$r_{\max} = 100, \lambda = 1.3, N = 100,$$

and the state weighting matrix was chosen as

$$Q = \mathbf{diag}(1, 0).$$

The ellipsoids are shown in Fig. 3-3 and the system states and control are shown for an initial condition of $x_0 = [2 \ 0]^T$ in Fig. 3-4.

Note that the control effort is highly nonlinear when the state approaches the origin. The proximity to the origin allows for a high gain to be used resulting in a sharp convergence, with no overshoot. Also, the control is inherently rough due to the

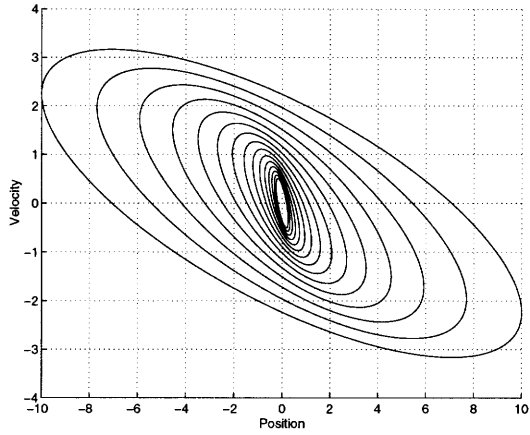


Figure 3-3: Nested Ellipsoids for Double Integrator

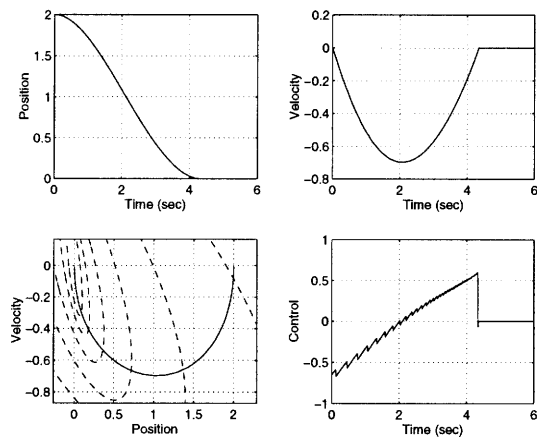


Figure 3-4: States and Control for Double Integrator

switchings that occur when the trajectory crosses from one ellipsoid to another. This can be reduced by adding more ellipsoids, but this results in a higher computation and storage burden. Indeed, the choice of the number of ellipsoids to use is somewhat subjective. As noted in [81] most of the advantage of the controller can be achieved through as few as five ellipsoids. It was also shown in [82] that an interpolation function can be used to smooth the control. The interpolation function has the additional advantage that it can be used to reduce the number of ellipsoids by taking a more spread out distribution, *i.e.*, an increased λ .

For a second order system such as this it is even possible to analytically compute the solution to the Riccati equation and the resulting gain as,

$$\begin{aligned}
 P(r) &= \begin{bmatrix} \sqrt{2}r^{1/4} & \sqrt{r} \\ \sqrt{r} & \sqrt{2}r^{3/4} \end{bmatrix} \\
 K(r) &= [r^{-1/2} \quad \sqrt{2}r^{-1/4}] \\
 \tilde{P}(r) &= \begin{bmatrix} \sqrt{2}r^{-1} & \sqrt{2}r^{-3/4} \\ \sqrt{2}r^{-3/4} & 2r^{-1/2} \end{bmatrix}.
 \end{aligned} \tag{3.17}$$

3.1.2 Limit Properties of Invariant Ellipsoids

An important consideration for the control methodology, from the standpoint of stability, is the limit properties of Ω . In the proof of Theorem 3.1 we have seen that global stability is guaranteed because the ellipsoids can be made arbitrarily large, *i.e.*,

$$\lim_{r \rightarrow \infty} \mathcal{E}(P(r), \alpha(r)) = \mathbf{R}^n.$$

This is provided by Assumption 2.1 that guarantees the system is globally controllable. For unstable systems it is not possible to obtain global stability and the outer most ellipsoid will approach a limiting shape, as in Fig. 3-5 for an unstable pendulum.

In the converse direction it is important that as $r \rightarrow 0$ the ellipsoids, corresponding to the increasingly aggressive gains $K(r)$, uniformly decrease to the origin. If this were not the situation one could imagine a case where the gains become increasingly large and the state is not driven to the equilibrium. The following lemma asserts a

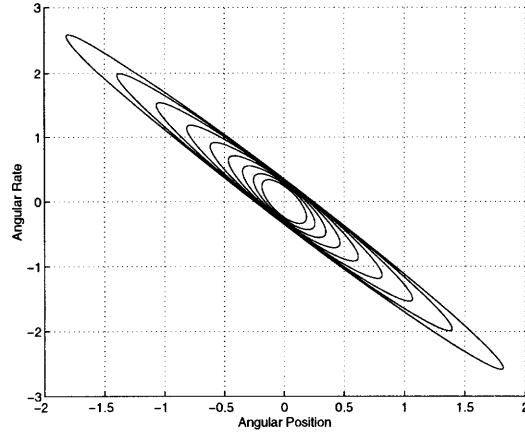


Figure 3-5: Open Loop Unstable System

condition under which the ellipsoids must uniformly collapse to the equilibrium.

Lemma 3.3 *Let Assumption 2.1 and 2.2 hold. If the state weighting matrix, Q , is positive definite then the largest diameter, in the standard Euclidian sense, of $\mathcal{E}(P(r), \alpha(r))$ approaches zero as r approaches zero.*

Proof: By Contradiction.

Assume that $Q > 0$ and the largest diameter, in the Euclidian sense, of $\mathcal{E}(P(r), \alpha(r))$ does not approach zero as r goes to zero. Then it follows that there exists an x^* such that $\|x^*\| > 0$ and

$$x^* \in \bigcap_{r \in \bar{\mathbf{R}}_+} \mathcal{E}(P(r), \alpha(r)).$$

Indeed, consider any infinite sequence $\infty > r_1 > r_2 > \dots > r_n > \dots$, where $\lim_{n \rightarrow \infty} r_n = 0$. Then, by the hypothesis, there exists a sequence $x_1, x_2, \dots, x_n, \dots$ such that $x_l \in \mathcal{E}(P(r_l), \alpha(r_l))$, and $\|x_l\| \geq m \neq 0$ ($l = 1, \dots, n, \dots$). Now, the first ellipsoid $\mathcal{E}(P(r_1), \alpha(r_1))$ covers a bounded domain because $P(r_1) > 0$ and $\infty > r_1$. Thus, the set of all x_l is bounded above and below, that is there exists M and m such that, $M \geq \{\|x_1\|, \|x_2\|, \dots, \|x_n\|, \dots\} \geq m \neq 0$. It follows from the Bolzano-Weierstrass theorem that we can find a subsequence $r_{\sigma(1)}, r_{\sigma(2)}, \dots, r_{\sigma(l)}, \dots$ such that

$x_{\sigma(1)}, x_{\sigma(2)}, \dots, x_{\sigma(l)}, \dots$ in the limit tends towards some x^* where

$$x^* \in \bigcap_{l \in [1, \infty)} \mathcal{E}(P(r_{\sigma(l)}), \alpha(r_{\sigma(l)})),$$

and $\|x^*\| \geq m$. From the definition of $\alpha(r)$ in (3.5) we obtain

$$x^{*T} P(r) x^* \frac{b_i^T P(r) b_i}{r^2} \leq x^{*T} P(r) x^* \max_i \frac{b_i^T P(r) b_i}{r^2} \leq 1, \quad (3.18)$$

for any r and i , where b_i is the i th column of the B matrix. It follows that for any value of i and r that

$$(P^{\frac{1}{2}} b_i)^2 (P^{\frac{1}{2}} x^*)^2 \leq r^2,$$

and by the Cauchy-Schwarz inequality

$$x^{*T} P b_i b_i^T P x^* \leq r^2.$$

Finally, from (3.4) we have

$$x^{*T} (A^T P + P A) x^* - \frac{x^{*T} P B B^T P x^*}{r} + x^{*T} Q x^* = 0,$$

which is equivalent to

$$x^{*T} (A^T P + P A) x^* - \sum_{i=1}^m \frac{x^{*T} P b_i b_i^T P x^*}{r} + x^{*T} Q x^* = 0.$$

Therefore

$$x^{*T} (A^T P + P A) x^* + x^{*T} Q x^* \leq m r.$$

Now from the continuity of α in Lemma 3.2 as $r \rightarrow 0$, $P(r) \rightarrow 0$ and thus

$$x^{*T} Q x^* \leq 0.$$

However, the initial assumption was $Q > 0$ and since $\|x^*\| \geq m$ we have a contradiction and the diameter of the ellipsoids must go to zero along all axes for $Q > 0$.

■

This provides the important corollary.

Corollary 3.1 *Let the assumptions of Lemma 3.3 hold. Consider the sequence*

$$\{r_1, r_2, \dots, r_n, \dots\},$$

with $r_i > r_j$ for $i < j$, and $\lim_{n \rightarrow \infty} r_n = 0$. Then the corresponding gains

$$\{K(r_1), K(r_2), \dots, K(r_n), \dots\}$$

will drive the state closer and closer to the origin. That is

$$\limsup_{t \rightarrow \infty} \|x(t)\| \rightarrow 0, \text{ as } r \rightarrow 0.$$

Even though in practice only a finite number of ellipsoids is used this property is still important to the control methodology. Indeed, it guarantees that the system state can be driven arbitrarily close to the equilibrium.

3.2 Asymmetric Controls

The simplest way to solve the asymmetric control problem is to once again make the position constraints symmetrical by using

$$|\underline{u}_i| = |\bar{u}_i| = \min\{|\underline{u}_i|, |\bar{u}_i|\}, \quad i = 1, \dots, m,$$

and reconstructing the controller accordingly. Obviously, this ignores a possibly large region of usable control that could result in poor convergence properties. In [82] the authors resolve the asymmetric control problem by independently scaling the gains, $K(r)$, to meet the position constraints in the two half-spaces of the ellipsoid corresponding to $K(r)x \leq 0$ and $K(r)x \geq 0$.

The following is a generalization of the method presented in [65]. Note that the

position constraints (2.22) can be normalized, as discussed in Section 2.3, such that $\bar{u}_i - \underline{u}_i = 2$, $i = 1, \dots, m$. Now define the new set of controls v_i such that,

$$u_i = v_i + \tilde{u}_i, \quad i = 1, \dots, m,$$

where,

$$\tilde{u}_i = (\bar{u}_i + \underline{u}_i)/2.$$

Thus, the asymmetrical bounds (2.22) on u are equivalent to the symmetrical bounds on v :

$$-1 \leq v_i \leq 1, \quad i = 1, \dots, m. \quad (3.19)$$

The problem is not as simple as creating a symmetrical controller for v as in the previous section. The difficulty lies in the fact that we have added a feedforward input to the control that will drive the system to a state that is not the origin. What we have done is to reduce the problem to a control that is symmetrical about an induced trim point

$$\tilde{a} = -A^{-1}B\tilde{u},$$

where $\tilde{u} = [\tilde{u}_1 \dots \tilde{u}_m]^T$, that is obtained by setting $\dot{x} = 0$ and $u = \tilde{u}$ in (2.18). However, we desire to return to the origin, $x = 0$. Note that this can be accomplished by first leading the trajectory to \tilde{a} and then progressively driving it to the origin along the set of points

$$a(\gamma) = -A^{-1}B\tilde{u}\gamma, \quad \gamma \in [1 \ 0],$$

where each $a(\gamma)$ is a trim point of the system. For each $a(\gamma)$ the control constraints on u can be satisfied by using invariant ellipsoids of the form $\mathcal{E}(P(r), \alpha(r)\gamma^2, a(\gamma))$, where γ is a scaling factor that reduces the size of each ellipsoid to satisfy the control constraints and maintain nesting. Note that this will automatically result in an ellipsoid of zero volume centered at the origin. Essentially we are using the trim space,

$$X_e = \{x \in \mathbf{R}^n : x = -A^{-1}B\tilde{u}\gamma, \text{ and } \gamma \in [1 \ 0]\},$$

where γ parameterizes the set, to control the system. Note that we can establish an ellipsoidal bound on X_e by considering

$$r_{\min} = \min r : X_e \subset \mathcal{E}(P(r_{\min}), \alpha(r_{\min}), a(1)),$$

and this value can be found by solving the equation

$$\alpha(r_{\min}) = \tilde{u}^T B^T A^{-T} P(r_{\min}) A^{-1} B \tilde{u}.$$

In other words r_{\min} defines the ellipsoid that is a tight bound on the trim space.

Note that explicit in this development is the assumption that the A matrix is non-singular. This is a limitation of the construction that follows. In certain cases where the A matrix is singular this problem can be avoided by removing the integrator state. However, in cases where this is not possible the method presented here cannot be used. Given that the A matrix is non-singular the following provides a construction under which the asymmetric control problem can be solved.

Theorem 3.2 *Let Assumptions 2.1 and 2.2 hold, and assume $\text{rank}(A) = n$. Consider the control $u = v + \tilde{u}$ with,*

$$v = -K(r)\tilde{x} + \tilde{u}(\gamma - 1), \quad \gamma \in [1 \ 0], \quad (3.20)$$

where $\tilde{x} = x - a(\gamma)$, with $K(r)$ the solution to (3.4) for $r \in \bar{\mathbf{R}}_+$. Let

$$r(x(t)) = \begin{cases} \min r : x(t) \in \mathcal{E}(P(r), \alpha(r), a(1)) & \text{if } x \ni \mathcal{E}(P(r_{\min}^+), \alpha(r_{\min}^+), a(1)) \\ r_{\min}^+ & \text{for } x \in \mathcal{E}(P(r_{\min}^+), \alpha(r_{\min}^+), a(1)), \end{cases} \quad (3.21)$$

where r_{\min}^+ is any value of $r > r_{\min}$. Define,

$$\gamma(r) = \begin{cases} 1 & r > r_{\min}^+ \\ \min \gamma : x \in \mathcal{E}(P(r_{\min}^+), \alpha(r_{\min}^+)\gamma^2, a(\gamma)) & r = r_{\min}^+. \end{cases} \quad (3.22)$$

Then the control u solves problem 2.

Proof: The proof consists of showing that the ellipsoid $\mathcal{E}(P(r), \alpha(r)\gamma^2, a(\gamma))$ is invariant for all r and γ , the control constraints are satisfied, and the ellipsoids are nested.

a) *Invariance:* Note that $V = \tilde{x}^T P(r) \tilde{x}$ is a Lyapunov function for the system (2.18) under the control (3.20) that guarantees the point $x = a(\gamma)$ is asymptotically stable.

b) *Constraint Satisfaction:* Indeed,

$$\max v_i = -k_i(r)\tilde{x} + \tilde{u}_i(\gamma - 1), \quad i = 1, \dots, m$$

subject to

$$\tilde{x}^T P(r) \tilde{x} = \alpha(r)\gamma^2$$

is

$$v_{\max_i} = \sqrt{\alpha(r)\gamma} \sqrt{k_i(r)P(r)k_i^T(r)} + \tilde{u}_i(\gamma - 1).$$

Consider the only two possible cases,

1. $\alpha(r) = 1/(k_i(r)P(r)k_i^T(r))$ for which the maximum is

$$|v_{\max_i}| = |-\tilde{u}_i + \gamma(1 + \tilde{u}_i)| \leq 1,$$

due to the fact that $|\tilde{u}_i| \leq 1$ and $\gamma \in [1 \ 0]$.

2. $\alpha(r) \neq 1/(k_i(r)P(r)k_i^T(r))$, but

$$\sqrt{k_i P k_i^T \alpha} = \beta < 1$$

and,

$$|v_{\max_i}| = |-\tilde{u}_i + \gamma(\beta + \tilde{u}_i)| \leq 1.$$

Thus, $|v_i| \leq 1$ and since $u = -K(r)\tilde{x} + \gamma\tilde{u}$ we will always have,

$$\underline{u}_i \leq u_i \leq \bar{u}_i, \quad i = 1, \dots, m.$$

c) *Nesting*: First, the ellipsoids $\mathcal{E}(P(r), \alpha(r), a(1)) \supset \mathcal{E}(P(r_{\min}^+), \alpha(r_{\min}^+), a(1))$ for $r > r_{\min}^+$ are all centered around $a(1)$, and the original nesting property applies. Now the the following shows that for $r = r_{\min}^+$, $\mathcal{E}(P(r_{\min}^+), \alpha(r_{\min}^+)\gamma_1^2, a) \subset \mathcal{E}(P(r_{\min}^+), \alpha(r_{\min}^+)\gamma_2^2, a)$, if $\gamma_1 < \gamma_2$. Consider the ellipsoids,

$$\mathcal{E}(\tilde{P}, \gamma_i^2, a_i(\gamma_i)), \quad i = 1, 2, \quad (3.23)$$

where $\tilde{P} = P/\alpha(r_{\min}^+)$.

Using the linear transformation $T : x \rightarrow y$ defined by, $y = \tilde{P}^{1/2}x$ (3.23) becomes,

$$\mathcal{E}(\tilde{P}, \gamma_i^2, c_i),$$

where $c_i = \tilde{P}^{1/2}a_i$. A necessary and sufficient condition for $\mathcal{E}(\tilde{P}, \gamma_1^2, c_1) \subset \mathcal{E}(\tilde{P}, \gamma_2^2, c_2)$, and likewise for $\mathcal{E}(\tilde{P}, \gamma_1^2, a_1) \subset \mathcal{E}(\tilde{P}, \gamma_2^2, a_2)$, (because the transformation is linear) is,

$$\left\| (c_2 - c_1) + \frac{(c_2 - c_1)\gamma_1}{\|c_2 - c_1\|} \right\| \leq \gamma_2. \quad (3.24)$$

Letting $z = c_2 - c_1$ and expanding (3.24) we obtain,

$$(z^T z + 2(z^T z)^{1/2}\gamma_1 + \gamma_1^2)^{1/2} \leq \gamma_2.$$

Substituting $c_i = -\tilde{P}^{1/2}A^{-1}B\tilde{u}\gamma_i$ into the above

$$(\rho(\gamma_2 - \gamma_1)^2 + 2\sqrt{\rho(\gamma_2 - \gamma_1)^2\gamma_1 + \gamma_1^2})^{1/2} \leq \gamma_2,$$

where $\rho = \tilde{u}^T B^T A^{-T} \tilde{P} A^{-1} B \tilde{u}$. Simplifying this we obtain

$$[\sqrt{\rho}(\gamma_1 - \gamma_2) + \gamma_2] \leq \gamma_1.$$

Which is satisfied if and only if $\sqrt{\rho} \leq 1$. Now note that $\rho = 1$ corresponds to the ellipsoid, $\mathcal{E}(P(r_{\min}), \alpha(r_{\min}), a(1))$, that contains the trim space X_e and $\rho \leq 1$ corresponds to $r > r_{\min}$. Thus nesting property can be maintained by holding $r = r_{\min}^+$

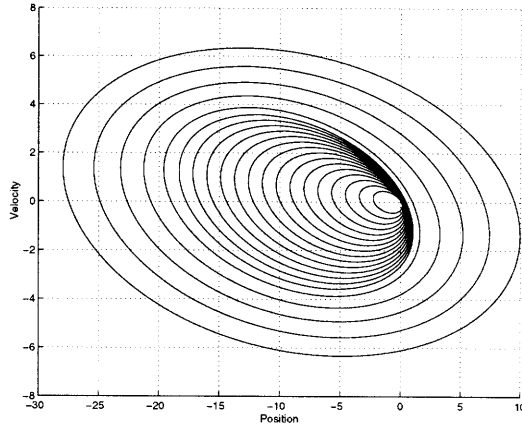


Figure 3-6: Asymmetric Ellipsoids for Spring Mass System

constant for ellipsoids in the trim space and γ can be chosen as any value on the interval $[1 \ 0]$. Furthermore, it is easy to see that the origin will always be contained in the interior of every ellipsoid. This is the reason we take $r_{\min}^+ > r_{\min}$.

Thus a trajectory starting in any ellipsoid will proceed towards the next inner ellipsoid and asymptotic stability and boundedness is guaranteed for all time. ■

The introduction of the induced trim point allows the regulation of a system with asymmetric input bounds to be accomplished by the introduction of a progressive feedforward gain. Trajectories starting far from the origin are first guided towards the induced trim point, \tilde{a} . Then once the trajectory enters the ellipsoid that contains the trim space it is then led progressively towards the origin. The obvious disadvantage is that there is a minimum value of the control weight, r , that can be used. Several methods were attempted to remove this constraint by using trim points that were functions of r , but it seems that it is difficult to maintain nesting and the control constraints at the same time. We will now give a simple example of this construction.

3.2.1 Example of Asymmetric Control

Consider the second order spring mass system

$$A = \begin{bmatrix} 0 & 1 \\ -0.1 & 0 \end{bmatrix}, \quad B = \begin{bmatrix} 0 \\ 1 \end{bmatrix}, \quad (3.25)$$

Example	APLC	HPB/AC
1	30s	21.6s
2	17.8s	12.2s

Table 3.1: 3% Settling Times for Asymmetric Control Examples

with the asymmetric input bounds

$$\underline{u}_i = -1.9, \bar{u}_i = 0.1.$$

The value for r_{\min} was computed as 106. Note that the control limits imply a value of $\tilde{u} = -0.9$, and the equivalent problem is that of regulating about the reference point $x^* = 9$. The control law construction parameters were chosen as

$$r_{\max} = 400, \lambda = 1.1, N = 100,$$

and the state weighting matrix was chosen as

$$Q = \mathbf{diag}(1, 1).$$

Fig. 3-6 shows the asymmetric ellipsoids for this particular example. Fig. 3-7 and 3-8 show the states and control for the two initial conditions $x_0 = [5 \ 0]^T$ and $x_0 = [-20 \ 0]^T$. The solid line represents the HPB with Asymmetric Constraints (HPB/AC). The dashed line is the performance of the Asymmetric PLC (APLC) controller in [82], shown for comparison. The performance of the two constructions is quite different in nature. The gain scaled controller seems to use the control effort more efficiently, but has a long convergence to the origin. Conversely the asymmetric controller has a large amount of overshoot in Fig. 3-7, but has better convergence properties in both cases. This is reflected in the times to settle to within 3% of the initial value that are shown in Table 3.1.

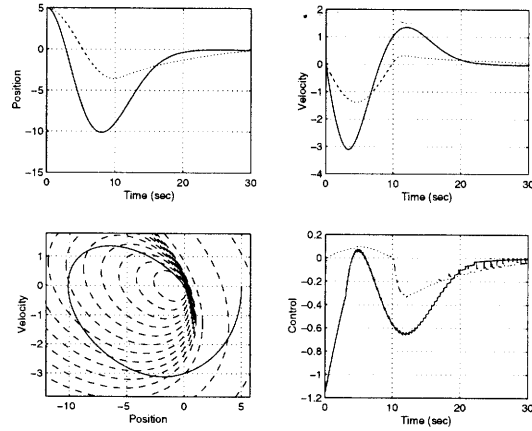


Figure 3-7: States and Control for Spring Mass System: Example 1

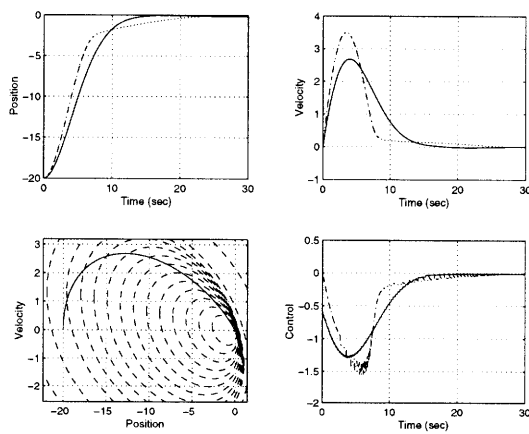


Figure 3-8: States and Control for Spring Mass System: Example 2

3.3 Position and Rate Constraints

3.3.1 LQR Based Solution

The process of adding symmetric rate constraints to the methodology begins by augmenting the state with the control as

$$\mathbf{x} = \begin{bmatrix} x \\ u \end{bmatrix}, \mathbf{A} = \begin{bmatrix} A & B \\ 0 & 0 \end{bmatrix}, \mathbf{B} = \begin{bmatrix} 0 \\ I_m \end{bmatrix}. \quad (3.26)$$

This leads to the differential equation for the augmented system,

$$\dot{\mathbf{x}} = \mathbf{A}\mathbf{x} + \mathbf{B}\dot{u}, \mathbf{x}(0) = \mathbf{x}_0. \quad (3.27)$$

The advantage to this formulation is that the problem has been placed in a structure similar to the NSFP. The control rate now appears as the system input, and the original control is now a state of the system. Thus, the constrained control and control rate problem can be seen as satisfying a control position constraint (formerly the rate constraint), and state constraint (formerly the control constraint) for the system (3.27). Following the introduction to this chapter we are now interested in the set

$$\mathcal{U}(K) = \mathcal{L}(K) \cap \mathcal{L}(C),$$

where

$$C = \begin{bmatrix} 0 \\ I_m \end{bmatrix} \quad (3.28)$$

represents the normalized control or state constraints. Again, $\mathcal{U}(K)$ represents the set of initial conditions for which the position and rate constraints will not be violated. Further, we have the maximal invariant set for a given K as

$$\mathcal{V}(K) = \bigcap_{t \in [0, \infty)} \left((e^{(A+BK)t})^{-1} \mathcal{U} \right). \quad (3.29)$$

The approach given here will be to approximate the set $\mathcal{V}(K)$ by means of an invariant ellipsoid within the framework of the methodology of Section 3.1. First we need a series of definitions.

For the system (3.27) we define the augmented Riccati equation arising from (3.3) (with $R = rI_m$) as

$$\mathbf{A}^T \mathbf{P} + \mathbf{P} \mathbf{A} - \frac{\mathbf{P} \mathbf{B} \mathbf{B}^T \mathbf{P}}{r} + \mathbf{Q} = 0, \quad (3.30)$$

with the \mathbf{P} and \mathbf{Q} matrices partitioned as

$$\mathbf{P} = \begin{bmatrix} P_{11} & P_{12} \\ P_{12}^T & P_{22} \end{bmatrix}, \quad \mathbf{Q} = \begin{bmatrix} Q_{11} & 0 \\ 0 & Q_{22} \end{bmatrix}, \quad (3.31)$$

such that $P_{11} \in \mathbf{R}^{n \times n}$, $P_{12} \in \mathbf{R}^{n \times m}$, $P_{22} \in \mathbf{R}^{m \times m}$, $Q_{11} \in \mathbf{R}^{n \times n}$, and $Q_{22} \in \mathbf{R}^{m \times m}$.

We will also define here the inverse of the \mathbf{P} matrix

$$\mathbf{M} = \mathbf{P}^{-1} = \begin{bmatrix} M_{11} & M_{12} \\ M_{12}^T & M_{22} \end{bmatrix}, \quad (3.32)$$

which satisfies the Riccati equation

$$\mathbf{A} \mathbf{M} + \mathbf{M} \mathbf{A}^T - \frac{\mathbf{B} \mathbf{B}^T}{r} + \mathbf{M} \mathbf{Q} \mathbf{M} = 0. \quad (3.33)$$

It will be necessary, in the following development, to have the constraints (2.23) normalized to ± 1 . Indeed, this can be accomplished, in all cases, by means of an input substitution and a state transformation. The input substitution

$$\dot{\hat{u}}_i = \frac{\dot{u}_i}{\hat{u}_i},$$

normalizes the rate constraints. From this the input matrix \mathbf{B} becomes

$$\mathbf{B}_S = \begin{bmatrix} 0 \\ \Phi \end{bmatrix}, \quad (3.34)$$

where $\Phi = \mathbf{diag}(\dot{u}_1, \dots, \dot{u}_m)$. The state transformation

$$T = \begin{bmatrix} I_n & 0 \\ 0 & \Psi \end{bmatrix}, \quad (3.35)$$

where $\Psi = \mathbf{diag}(1/\bar{u}_1, \dots, 1/\bar{u}_m)$, normalizes the position constraints. Combining the two transformations gives

$$\mathbf{A}_T = T\mathbf{A}T^{-1} = \begin{bmatrix} A & B\Psi^{-1} \\ 0 & 0 \end{bmatrix}, \quad (3.36)$$

$$\mathbf{B}_{TS} = T\mathbf{B}_S = \begin{bmatrix} 0 \\ \Psi\Phi \end{bmatrix}. \quad (3.37)$$

Thus, the system (3.27) can be transformed to an equivalent system with the position and rate constraints normalized as

$$|u_i| \leq 1, \quad |\dot{u}_i| \leq 1, \quad i = 1, \dots, m. \quad (3.38)$$

In the following, the subscripts of the transformed matrices will be dropped for notational convenience. The following theorem establishes a construction by which the normalized system can be globally asymptotically stabilized by means of a nonlinear state feedback.

Theorem 3.3 *Let Assumptions 2.1 and 2.2 hold. Assume that $Q_{11} = \Lambda \geq 0$ and $Q_{22}(r) = rI_m$, where $\Lambda \in \mathbf{R}^{n \times n}$. Then the control*

$$\dot{u} = -\frac{\mathbf{B}^T \mathbf{P}(r)}{r} \mathbf{x},$$

with $\mathbf{P}(r)$ the solution to (3.30) for $r \in \bar{\mathbf{R}}_+$, and

$$r(x(t)) = \min r : x(t) \in \mathcal{E}(\mathbf{P}(r), \alpha(r)), \quad \forall t,$$

with

$$\begin{aligned}\alpha(r) &= 1/\max(\text{diag}(K(r)\mathbf{P}^{-1}(r)K^T(r))) \\ &= 1/\max(\text{diag}(B^T\mathbf{P}(r)B/r^2)),\end{aligned}\tag{3.39}$$

solves Problem 3.

Proof: The proof consists of two parts. The first part is very similar to that of Theorem 3.1 and shows that there still exists a set of nested invariant ellipsoids for asymptotic stability. The second part shows that both the position and rate constraint can be satisfied for all time.

a) *Invariance and Nesting:* Note that

$$V = \mathbf{x}^T\mathbf{P}(r)\mathbf{x},$$

for any r , is a Lyapunov function for the closed loop system that is strictly decreasing along all trajectories. That is, once the trajectory enters $\mathcal{E}(\mathbf{P}(r), \alpha(r))$ it will stay there for all time. The nesting of the ellipsoids is then sufficient to prove that any trajectory starting in the set will asymptotically approach the equilibrium. The condition for nesting is ([81, 53])

$$\frac{d\tilde{\mathbf{P}}(r)}{dr} \leq 0,\tag{3.40}$$

where

$$\tilde{\mathbf{P}}(r) = \frac{\mathbf{P}(r)}{\alpha(r)},\tag{3.41}$$

and $\alpha(r)$ is defined by (3.39). It will now be shown that

$$\mathbf{Q}(r) - \frac{d\mathbf{Q}(r)}{dr}r \geq 0\tag{3.42}$$

is a sufficient condition for the ellipsoids to be nested, and that this is indeed satisfied by the construction of Theorem 3.3. Taking the derivative of (3.30) with respect to r

and collecting terms gives

$$\mathbf{A}_{\text{cl}}^T d\mathbf{P} + d\mathbf{P}\mathbf{A}_{\text{cl}} + \frac{\mathbf{P}\mathbf{B}\mathbf{B}^T\mathbf{P}}{r^2} dr + d\mathbf{Q} = 0, \quad (3.43)$$

where $\mathbf{A}_{\text{cl}} = \mathbf{A} - \frac{\mathbf{B}\mathbf{B}^T\mathbf{P}(r)}{r}$. Let $\tilde{\mathbf{b}}$ be the maximizer. Taking the derivative of $\tilde{\mathbf{P}}(r)$ with respect to r

$$d\tilde{\mathbf{P}}(r) = (\tilde{\mathbf{b}}^T\mathbf{P}\tilde{\mathbf{b}}) \frac{d\mathbf{P}}{r^2} + \frac{\tilde{\mathbf{b}}^T d\mathbf{P}\tilde{\mathbf{b}}\mathbf{P}}{r^2} - 2(\tilde{\mathbf{b}}^T\mathbf{P}\tilde{\mathbf{b}}) \frac{\mathbf{P}}{r^3} dr. \quad (3.44)$$

From (3.43) we can write

$$\frac{d\mathbf{P}(r)}{dr} = \int_0^\infty e^{\mathbf{A}_{\text{cl}}^T \tau} \left(\frac{\mathbf{P}\mathbf{B}\mathbf{B}^T\mathbf{P}}{r^2} + \frac{d\mathbf{Q}}{dr} \right) e^{\mathbf{A}_{\text{cl}}\tau} d\tau, \quad (3.45)$$

and from (3.30) \mathbf{P} satisfies

$$\mathbf{P}(r) = \int_0^\infty e^{\mathbf{A}_{\text{cl}}^T \tau} \left(\frac{\mathbf{P}\mathbf{B}\mathbf{B}^T\mathbf{P}}{r} + \mathbf{Q} \right) e^{\mathbf{A}_{\text{cl}}\tau} d\tau. \quad (3.46)$$

Substituting (3.45) and (3.46) into (3.44) we eventually obtain (after some manipulation)

$$\begin{aligned} d\tilde{\mathbf{P}}(r) = & - \left[\int_0^\infty e^{\mathbf{A}_{\text{cl}}^T \tau} \left(\mathbf{Q} - r \frac{d\mathbf{Q}}{dr} \right) e^{\mathbf{A}_{\text{cl}}\tau} d\tau \frac{\tilde{\mathbf{b}}^T\mathbf{P}\tilde{\mathbf{b}}}{r^3} \right. \\ & \left. + \tilde{\mathbf{b}}^T \int_0^\infty e^{\mathbf{A}_{\text{cl}}^T \tau} \left(\mathbf{Q} - r \frac{d\mathbf{Q}}{dr} \right) e^{\mathbf{A}_{\text{cl}}\tau} d\tau \tilde{\mathbf{b}} \frac{\mathbf{P}}{r^3} \right] dr. \end{aligned} \quad (3.47)$$

Thus, from (3.40), and the argument of Theorem 3.1 a sufficient condition for nesting is

$$\mathbf{Q}(r) - \frac{d\mathbf{Q}(r)}{dr} r \geq 0.$$

Now by assumption

$$\mathbf{Q}(r) - \frac{d\mathbf{Q}(r)}{dr} r = \begin{bmatrix} \Lambda & 0 \\ 0 & 0 \end{bmatrix} \geq 0, \quad (3.48)$$

and thus the nesting condition is satisfied via the same argument in Theorem 3.1. Global asymptotic stability for any admissible initial condition also follows from an argument similar to that in Theorem 3.1.

b) *Constraint Satisfaction*: The second part of the proof is to show that the position and rate constraints are satisfied. Indeed, the rate constraint is satisfied immediately from the scaling (3.41). The position constraint can be defined by the orthogonal slabs $\mathcal{H}(c_i)$ where c_i is the i th column of the matrix C in (3.28). The ellipsoid $\mathcal{E}(\tilde{\mathbf{P}}(r), \alpha(r))$ will be contained within the slabs $\mathcal{H}(c_i), i = 1, \dots, m$, if and only if

$$\text{diag}(C^T \tilde{\mathbf{P}}^{-1}(r) C) \leq I_m.$$

This is equivalent to

$$\text{diag}(C^T \mathbf{P}^{-1}(r) C) \leq \frac{I_m}{\alpha},$$

and by definition of the block structure of $\mathbf{P}(r)$ and $\mathbf{M}(r)$ this is equivalent to

$$\text{diag}(M_{22}(r)) \leq \max \left(\text{diag} \left(\frac{\Phi \Psi P_{22}(r) \Psi \Phi}{r^2} \right) \right) I_m, \quad (3.49)$$

and

$$\text{diag}(M_{22}(r)) \leq \max(\text{diag}(P_{22}(r))) \frac{\Phi^2 \Psi^2}{r^2}. \quad (3.50)$$

The next step is to show that (3.50) is satisfied by the construction outlined in Theorem 3.3. Indeed, according to the block structure of (3.31) and (3.32), the Riccati equation (3.33) can be written block by block to give

$$-\frac{\Psi^2 \Phi^2}{r} + M_{12}^T M_{12} + M_{22}^2 r = 0,$$

and

$$M_{22}^2 = \frac{\Psi^2 \Phi^2}{r^2} - M_{12}^T M_{12}.$$

Therefore

$$M_{22}^2 \leq \frac{\Psi^2 \Phi^2}{r^2}. \quad (3.51)$$

At this point note the following Lemma, adapted from Lemma 7.5 in [55].

Lemma 3.4 *Suppose that $X \in \mathbf{R}^{m \times m}, Y \in \mathbf{R}^{m \times m}$, with $X = X^T > 0$, and $Y = Y^T > 0$. Let n be a positive integer. Then there exists matrices $X_2 \in \mathbf{R}^{n \times m}, X_1 \in$*

$\mathbf{R}^{n \times n}$ such that $X_1 = X_1^T$, and

$$1. \begin{bmatrix} X_1 & X_2 \\ X_2^T & X \end{bmatrix} > 0 \quad (3.52)$$

$$2. \begin{bmatrix} X_1 & X_2 \\ X_2^T & X \end{bmatrix}^{-1} = \begin{bmatrix} ? & ? \\ ? & Y \end{bmatrix} \quad (3.53)$$

if and only if $X - Y^{-1} \geq 0$, and $\text{rank}(X - Y^{-1}) \leq n$.

Since $\mathbf{P}(r)$ is positive definite we get

$$P_{22}(r) \geq M_{22}^{-1}(r).$$

Combining this with (3.51) we obtain

$$M_{22}(r) \leq \frac{P_{22}(r)\Psi^2\Phi^2}{r^2},$$

and

$$\text{diag}(M_{22}(r)) \leq \text{diag}(P_{22}(r)) \frac{\Psi^2\Phi^2}{r^2},$$

by virtue of the fact that for $A \geq 0, B \geq 0$, $A \leq B$ implies $\text{diag}(A) \leq \text{diag}(B)$. Thus the condition (3.50) is satisfied. This guarantees that the position constraint is always satisfied. Thus stability and boundedness of the position and rate constraints is guaranteed and the theorem is proven. \blacksquare

This construction is equivalent to modifying the original LQR cost (3.3) to include the control rate as

$$J = \int_0^\infty (\mathbf{x}^T Q_{11} \mathbf{x} + r u^T u + r \dot{u}^T \dot{u}) dt. \quad (3.54)$$

Implicit in all of this is the fact that the position and rate bounds are normalized to ± 1 . It is not immediately obvious why this normalization is necessary. Indeed, consider the case where one of the control inputs has one value for its position limit and another for its rate limit. The fundamental property of the construction is that

the control and control rate planes become parallel as $r \rightarrow \infty$. If they are not normalized there will be no way to satisfy both simultaneously. It is also important to note that among the class of functions $Q_{22}(r) = ar^b I_m$ the choice of $Q_{22}(r) = r I_m$ is optimal. Indeed, it can be seen immediately that the nesting condition (3.42) requires $b \leq 1$. Furthermore, the condition (3.50) implies that $b \geq 1$ and $a \geq 1$. Now note that for $a \geq 1$ the rate planes will fail to become aligned with the position constraint.

The following provides a simple example to illustrate the method developed in this section.

Single Integrator Example

In order to visualize the construction of Section 3.3 in two dimensions a controller will be synthesized for the single state system

$$A = 0, \quad B = 1, \quad |u| \leq 1, \quad |\dot{u}| \leq 1. \quad (3.55)$$

This leads to the augmented form

$$\mathbf{A} = \begin{bmatrix} 0 & 1 \\ 0 & 0 \end{bmatrix}, \quad \mathbf{B} = \begin{bmatrix} 0 \\ 1 \end{bmatrix}. \quad (3.56)$$

The ellipsoidal set, shown in Fig. 3-9 for $r_{\max} = 50000$, is quite clearly contained within the position constraint ± 1 for all values of r . More importantly, note that the rate plane is almost tangent to the position constraint. Following the discussion above, if the control and control rate are not penalized at the same value either the position constraint will be violated, or the construction will be unnecessarily conservative.

Unfortunately, it turns out this construction does not yield very good performance. An example of the performance for the initial condition $\mathbf{x} = [10 \ 0]^T$ is shown in Fig. 3-10 for the single integrator system. The regulation time for the HPB with Rate Constraints (HPB/RC) is long, and both the control and control rate are very under

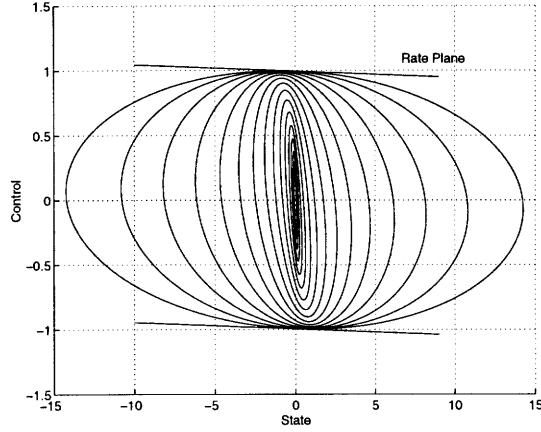


Figure 3-9: Invariant Ellipsoid Set for Single Integrator

utilized. Indeed, the time optimal controller is given by:

$$\dot{u} = \begin{cases} -\text{sign}(x_0) & 0 \leq t \leq 1 \\ 0 & 1 < t \leq x_0 \\ \text{sign}(x_0) & x_0 < t \leq x_0 + 1 \end{cases} . \quad (3.57)$$

For the initial condition $\mathbf{x} = [10 \ 0]^T$ the minimum time to reach the origin is $t = 11\text{s}$, substantially faster than that shown in Fig. 3-10.

Limit Properties of State Constrained Ellipsoids

A serious question is the limit properties of the construction in Theorem 3.3. As $r \rightarrow \infty$ the control rate hyperplane approaches $\mathbf{K} = [0 \ 1]$. Then, given that the system is ANCBC the region of invariance will approach an infinite slab. In the converse direction we have

Lemma 3.5 *Let Assumption 2.1 and 2.2 hold. If the state weighting matrix, Q_{11} , is positive definite then the largest diameter, in the standard Euclidian sense, of $\mathcal{E}(P_{11}(r), \alpha(r))$ approaches zero as r approaches zero.*

Proof: Following the proof of Lemma 3.3 we assume that Q_{11} is positive definite and the diameter of $\mathcal{E}(P_{11}(r), \alpha(r))$ does not go to zero. This implies that there exists

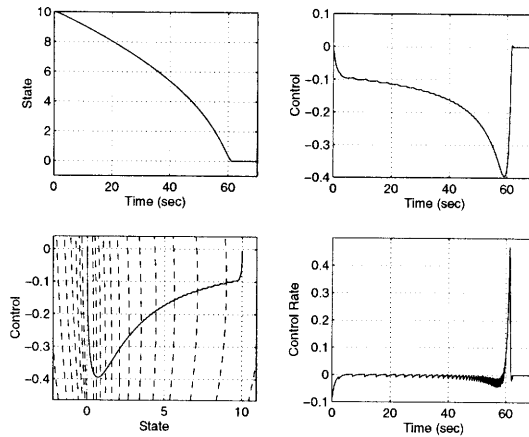


Figure 3-10: Performance of Single State System

an $\mathbf{x}^* = [x^{*T} 0]^T$ that is contained in the union of the ellipsoids $\mathcal{E}(\mathbf{P}(r), \alpha(r))$ over all r . We can then show that this leads to a contradiction and that the largest diameter of $\mathcal{E}(P_{11}(r), \alpha(r))$ must go to zero. ■

In other words, this implies that we still have state convergence, but not necessarily convergence of the control. Indeed, we do not want the control to be limited at any point, but we do want the state to always be driven closer and closer to the origin. It should then be apparent that in order to obtain the best performance the ellipsoids should have very little rotation and always contain as much of the control state axes as possible. There is very little flexibility over the shape of the matrix $\mathbf{P}(r)$, and the consequence is that the resulting controllers based on this construction seem to be conservative. However it is possible to recover the performance of this construction by using Linear Matrix Inequalities (LMIs).

3.3.2 Performance Enhancements via LMIs

The construction of Theorem 3.3 does not meet one of the primary objectives, namely, performance. The geometric constraints are satisfied, but the region of stabilization generated is highly conservative. In other words for a given value of r the ellipsoid generated by the Riccati equation solution matrix $\mathbf{P}(r)$ does not yield a good ap-

proximation to the set $\mathcal{V}(K)$. Nevertheless, the characteristics of the gains, $\mathbf{K}(r)$, are what allow the simultaneous satisfaction of the position and rate constraints. Due to the excellent robustness properties of the Linear Quadratic Regulator it is likely that for a fixed value of r there exists a larger region over which the system can be stabilized, than the region generated by the construction in Theorem 3.3. Thus, for any given r , and hence $\mathbf{K}(r)$, the objective is to increase the region of stability as much as possible by solving an LMI problem. In other words we want to use the knowledge of Theorem 2.2 to obtain a better $\mathbf{P}(r)$ or $\mathbf{\Gamma}(r)$.

Formulation of an LMI problem consists of choosing the desired objective and constraints. The position and rate constraints are easily described by following linear inequalities in $\mathbf{\Gamma}(r)$

$$\begin{aligned} \text{diag}(C^T \mathbf{\Gamma}(r) C) &\leq I_m, \\ \text{diag}(\mathbf{K}(r) \mathbf{\Gamma}(r) \mathbf{K}^T(r)) &\leq I_m, \end{aligned} \tag{3.58}$$

where

$$C = \begin{bmatrix} 0 \\ I_m \end{bmatrix}. \tag{3.59}$$

For $r_1 > r_2$, $r_i \in \mathcal{R}$ the nesting condition is ([81])

$$\mathbf{\Gamma}(r_1) - \mathbf{\Gamma}(r_2) > 0. \tag{3.60}$$

We then desire to solve an LMI problem for each value of r . Thus, where as all of the previous constructions were continuous in r , $\mathbf{\Gamma}(r)$ will only be valid where it can be computed. A straightforward and logical objective would be to maximize the volume of $\mathbf{\Gamma}(r)$. This yields the LMI problem

$$\begin{aligned} &\text{maximize } \log \det \mathbf{\Gamma}(r) \\ &\text{subject to (3.58,3.60),} \end{aligned}$$

which is a determinant maximization problem.

Maximizing the volume of $\mathbf{\Gamma}(r)$ does not necessarily yield the best performance. As was observed from the simple example above, one would expect that the ellipsoids

should, ideally, have one axis perpendicular to each of the position constraints in order to allow for the maximum possible control effort. Indeed, we wish to add some parameters into the optimization that will allow us to adjust the shape of the ellipsoids. From the perspective of performance there are really two points of interest. The first is the degree to which each ellipsoid is tangent to the control rate hyperplanes, where by degree of tangency we mean the

$$\min \|x - y\| : x \in \mathcal{P}(\mathbf{k}_i^T(r)), y \in \mathcal{E}(\mathbf{P}(r), \alpha(r)),$$

that is, the smallest distance from the ellipsoid boundary to the hyperplane. The second is the degree of tangency with the the point c_i , where c_i is the i th column of the C matrix. The former of the two can be accomplished by means of the constraint

$$\Delta \leq \text{diag}(\mathbf{K}(r)\mathbf{\Gamma}(r)\mathbf{K}^T(r))$$

where Δ is a diagonal matrix variable for which the $\text{Tr}(\Delta)$ needs to be maximized. The second objective can be accomplished by forcing the ellipsoid as close as possible to the points c_i . This constraint can be represented as

$$c_i^T \mathbf{\Gamma}^{-1}(r) c_i \leq \delta_i, \quad i = 1, \dots, m$$

where the δ_i are variables to be minimized. This constraint is not linear in Γ , but we note that using the example in Section 2.1.1 this is equivalent to

$$\begin{bmatrix} \mathbf{\Gamma}(r) & c_i \\ c_i^T & \delta_i \end{bmatrix} > 0, \quad (3.61)$$

by use of Schur complements.

All of this is summarized in the following construction algorithm.

Algorithm 1

1. Select a value for r_{\max} (defines the outer most ellipsoid), the desired number of

ellipsoids N , and λ . Let l denote the ellipsoid number. Set $l = 1$ and $r_1 = r_{\max}$.

2. Solve for $\mathbf{K}(r_l)$ from (3.30) with $\mathbf{Q}(r)$ as in Theorem 1.
3. Solve the following LMI problem.

$$\text{maximize: } \log \det \mathbf{\Gamma}(r_l) + \alpha \text{Tr}(\Delta) - \beta \sum_{i=1}^m \delta_i$$

subject to:

$$\Delta > 0$$

$$\begin{bmatrix} \mathbf{\Gamma}(r_l) & c_i \\ c_i^T & \delta_i \end{bmatrix} > 0, \quad i = 1, \dots, m$$

$$\Delta \leq \text{diag}(\mathbf{K}(r_l)\mathbf{\Gamma}(r_l)\mathbf{K}^T(r_l)) \leq I_m$$

$$\text{diag}(C^T\mathbf{\Gamma}(r_l)C) \leq I_m$$

$$\mathbf{A}_{\text{cl}}\mathbf{\Gamma}(r_l) + \mathbf{\Gamma}(r_l)\mathbf{A}_{\text{cl}}^T < 0$$

where $\mathbf{A}_{\text{cl}} = (\mathbf{A} + \mathbf{B}\mathbf{K}(r))$, and α and β are tunable parameters that reflect the desired trade off between ellipsoid volume and satisfaction of the position and rate constraints.

4. Set $r_{l+1} = \frac{r_l}{\lambda}$
5. Add the nesting constraint,

$$\mathbf{\Gamma}(r_{l-1}) - \mathbf{\Gamma}(r_l) > 0$$

to the the LMI in step 3, let $l = l + 1$, and repeat from step 2 until $l = N$.

It is important to note that, in practice, r_{\max} must be chosen quite large because lower values imply rate planes that are not tangent with the position constraints which can prematurely confine the above algorithm. Indeed, this is the reason the nesting constraint is not added prematurely. The following illustrates an example of this construction to the single state system described above.

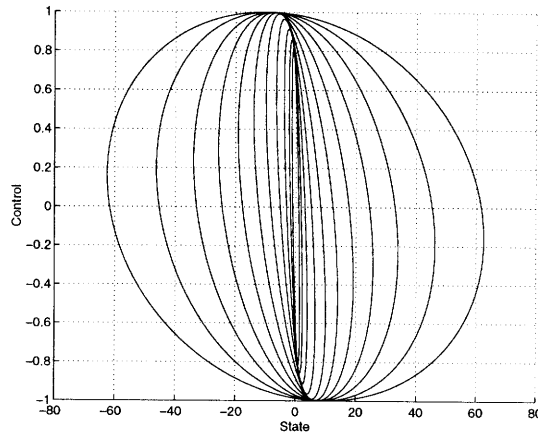


Figure 3-11: LMI Invariant Ellipsoid Set for Single Integrator

Single State System with LMI Enhancements

The algorithm of the previous section can be easily applied to the single state system (3.56). All of the LMI problems were solved with the software package [83]. Computational times were quite fast for this example, and a set of 50 ellipsoids took no more than a few minutes (real time) to calculate on a SUN SPARC 5 workstation. It is clear from Fig. 3-11 that the invariant set now covers a much larger region than Fig. 3-9, for the same value of $r_{\max} = 50000$. The value of $\alpha = 10$, and $\beta = 1$ were selected by trial and error, but simulations showed that the construction is not very sensitive to changes in these values. The performance, shown in Fig. 3-12, has been drastically improved to the point where the convergence time is approximately $t = 13.3s$ and is within a few seconds of the time optimal controller which yields the optimal value $t = 11s$.

3.4 Comparison with Reachable Sets

3.4.1 Sub-Reachable Sets

An important concept in systems and control theory is that of reachable sets. For each initial condition $x_0 \in \mathcal{X}_0 \subset \mathbf{R}^n$, there will exist multiple trajectories corresponding to

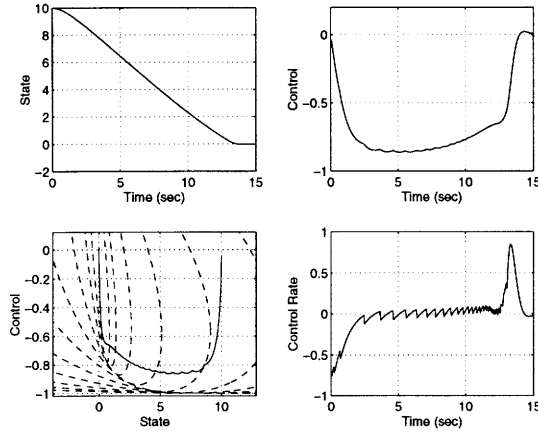


Figure 3-12: Performance of Single State system with LMI Enhancements

different control inputs. As expected, we will only be dealing with reachable sets for constrained systems. Consider the set of all possible end points of $x(t)$ at some time $t_f \geq 0$. We now provide the following definition.

Definition 3.1 ([17]) *The set of all endpoints of $x(t)$ at $t = t_f$ of all trajectories of the system (2.18) with $u \in \mathcal{U} \subset \mathbf{R}^m$, under the initial condition $x_0 \in \mathcal{X}_0$ is called the reachable set and denoted by $\mathcal{R}(t_f, \mathcal{X}_0)$.*

Reachable sets play a very fundamental role in control theory and a large number of basic control problems can be formulated in terms of them. Consider the problem of time optimal control. That is, given an initial condition $x_0 \in \mathcal{X}_0$, we must find an admissible control u such that the system reaches a certain set \mathcal{N} in the shortest possible time. In terms of reachable sets, the problem is to find the minimal time T such that the intersection between the reachable set and \mathcal{N} is non-empty, *i.e.*,

$$\mathcal{N} \cap \mathcal{R}(T, \mathcal{X}_0) \neq \emptyset$$

where \emptyset is the empty set. A good list of control problems that can be formulated in terms of reachable sets is given in [17].

As is often the case, it is impractical to analytically compute the reachable set for a system of more than second or third order. This leaves us with approximating them. Many methods exist for such approximation. We will be interested in a particularly interesting approximation known as the method of ellipsoids, first introduced by Chernousko. An extensive presentation of this method is the recent book [17].

In particular, consider the system (2.18) subject to the ellipsoidal input constraint

$$u \in \mathcal{E}^{-1}(U, 0)$$

(note that we are using the inverse ellipsoid \mathcal{E}^{-1} here that has a different representation, see the notation) and the initial conditions

$$x_0 \in \mathcal{E}^{-1}(Q_0, a_0).$$

Consider now the problem of obtaining estimates on the reachable set by means of sub-reachable and super-reachable ellipsoids. That is, we desire to find two ellipsoids $\mathcal{E}^{-1}(Q^-, a^-)$ and $\mathcal{E}^{-1}(Q^+, a^+)$ such that we have upper and lower geometrical bounds on the reachable set:

$$\mathcal{E}^{-1}(Q^-, a^-) \subset \mathcal{R}(t_f, \mathcal{E}^{-1}(Q_0, a_0)) \subset \mathcal{E}^{-1}(Q^+, a^+).$$

For control applications we will only be interested in the sub-reachable or inner approximation of the reachable set. The reason for this will become obvious in the following development. Chernousko showed that the differential equation for the maximal volume sub-reachable ellipsoidal approximation is

$$\begin{aligned} \dot{Q}^- &= AQ^- + Q^-A^T + 2(Q^-)^{1/2}[(Q^-)^{1/2}BUB^T(Q^-)^{1/2}]^{1/2}(Q^-)^{1/2} \\ Q^-(0) &= Q_0 \end{aligned} \tag{3.62}$$

and

$$\dot{a} = Aa, \quad a(0) = a_0.$$

This is a very useful equation, since it allows us to take any dynamical system with some set of initial conditions and admissible controls, and directly compute an approximation to the sub-reachable set via a differential equation. This knowledge can be directly applied to construction of a bounded feedback controller, and for that we define the dual to reachable sets known as controllable sets.

Definition 3.2 *The set of all points x such that the trajectories of the system (2.18) can be asymptotically stabilized to the origin with $u \in \mathcal{U} \subset \mathbf{R}^m$ in some finite time τ is called the controllable set and denoted by $\mathcal{C}(\tau, \mathcal{U})$*

In [37] Komarov showed that a family of sub-controllable sets for the NSFP problem is generated by $\mathcal{E}^{-1}(Q(\tau), 0)$ where $Q(\tau)$ is the solution to the differential equation

$$\frac{dQ(\tau)}{d\tau} = -AQ - QA^T + 2Q^{1/2}[Q^{1/2}BUB^TQ^{1/2}]^{1/2}Q^{1/2} \quad (3.63)$$

which is exactly the same as (3.62) with the system dynamics in reverse time ($A = -A$). This makes perfect sense, since we are now interested in controlling the system instead of analyzing it. From (3.63) we can define the minimal-time differentiable function $T(x)$

$$T(x) = \inf\{\tau \geq 0 : x \in \mathcal{E}^{-1}(Q(\tau), 0)\}$$

which due to the nature of the approximation is always larger than the time-optimal function $T_m(x)$, that is $T_m(x) \leq T(x)$ [37]. Furthermore, the function $T(x) = \tau$ is implicitly defined by the ellipsoids for each τ by solving the equation

$$x^T Q^{-1}(T(x))x = 1.$$

Finally, Komarov showed that the following control law solves the NSFP problem:

$$\begin{aligned} Bu &= K(x)x \\ K(x) &= -F(Q(T(x)))Q^{-1}(T(x)) \end{aligned} \quad (3.64)$$

where $F(Q) = Q^{1/2}[Q^{1/2}BUB^TQ^{1/2}]^{1/2}Q^{1/2}$.

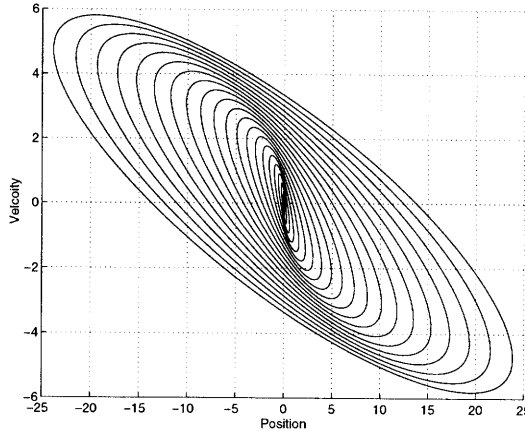


Figure 3-13: Sub-Controllable Set for Double Integrator

Notice the large number of similarities between this method and the one presented in the previous sections. Essentially, this is a sub-time-optimal nonlinear feedback controller whose gain is scheduled according to the state. The inner approximation is used to guarantee that the control constraints will not be violated. The most important difference between this controller and the one developed in Section 3.1 is that the control (3.64) guarantees convergence in finite time. As was noted in [70] the ellipsoids $\mathcal{E}^{-1}(Q(\tau), 0)$ form a nested invariant set in the same way as the construction in Theorem 3.1. The sub-controllable set and performance for the control (3.64) are shown in Figs. 3-13 and 3-14. This allows us to perform a comparison with the HPB controller in Fig. 3-4. Not surprising is the fact that the optimal ellipsoids do provide better performance. Indeed they comprise the maximal sub-optimal ellipsoids. However, to this authors knowledge, this approximation has not been extended to asymmetric and rate constrained systems.

3.4.2 Extension to Controllable Sets with State Constraints

The method described above is not capable of taking into account constraints on the system state. Indeed, this is the case when considering actuator rate constraints. Here, we will propose a preliminary method for accomplishing this through calculat-

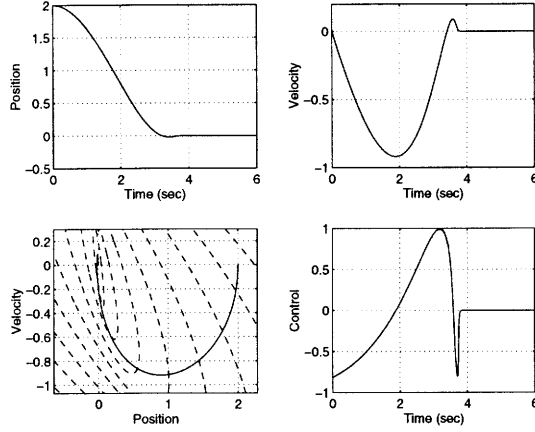


Figure 3-14: Performance for Sub-Controllable Set Controller

ing the maximal volume ellipsoid contained in the intersection of an ellipsoid and a hyperplane. We do this with the idea of using (3.63) to evolve the ellipsoids until they touch the state constraint, and then at each time τ take an approximation of the intersection of the two. It is important to note that this is a somewhat heuristic method that may not be the best possible. We will discuss this at the end of this section.

Consider the ellipsoid $\mathcal{E}^{-1}(Q, 0)$ and the hyperplane $\mathcal{H}(c)$. We desire to find an approximation of the intersection of these two sets, that is, find \tilde{Q} such that

$$\mathcal{E}^{-1}(\tilde{Q}, 0) \subset \mathcal{E}^{-1}(Q, 0) \cap \mathcal{H}(c). \quad (3.65)$$

Note that the intersection will always be non-empty, provided that $\mathcal{H}(c)$ has non-zero volume. Indeed there are two cases. The first and easiest case occurs when $cc^T < Q^{-1}$ and thus $\tilde{Q} = Q$. The second case requires the use of two transformations to turn the problem into one we can deal with. The first transformation defined by $x = Q^{1/2}y$ turns the ellipsoid into a ball and the hyperplane into

$$\mathcal{H}(Q^{1/2}c).$$

The second transformation is a rotation so that the normal of the hyperplane becomes parallel to one of the axes of the ball. Indeed there always exists a matrix V such that $V^T V = V V^T = I$ and $V^T Q^{1/2} c c^T Q^{1/2} V = \Lambda$ where Λ is a diagonal matrix that has zero eigenvalues along all directions except the one corresponding to the normal of the hyperplane $\mathcal{H}(c)$, *i.e.*,

$$\Lambda^{-1} = \mathbf{diag}(\dots, \frac{1}{c^T Q c}, \dots).$$

We can now define the maximum volume ellipsoid contained in the intersection as

$$D = I + \frac{1 - \gamma}{\gamma^2} \Lambda^{-1},$$

where $\gamma = c^T Q c$ and thus,

$$\tilde{Q} = Q^{1/2} V D V^T Q^{1/2} = Q + \frac{1 - \gamma}{\gamma^2} Q c c^T Q.$$

Thus, we can arrive at a two stage differential equation for the evolution of the ellipsoids. Let τ' be the time at which $\gamma = c^T Q c = 1$ ($\gamma = 1$ indicates that the ellipsoid and state constraint are touching), and let $Q(0) = 0$.

1. For $\tau \leq \tau'$,

$$\frac{dQ}{d\tau} = -A Q - Q A^T + 2 Q^{1/2} [Q^{1/2} B U B^T Q^{1/2}]^{1/2} Q^{1/2} \quad (3.66)$$

2. For $\tau > \tau'$

$$\frac{d\tilde{Q}}{d\tau} = Q' + \frac{\gamma'(\gamma - 2)}{\gamma^3} Q c c^T Q + \frac{1 - \gamma}{\gamma^2} (Q' c c^T Q + Q c c^T Q') \quad (3.67)$$

where $(\cdot)'$ denotes the derivative with respect to τ and Q' is given by

$$\frac{dQ'}{d\tau} = -A \tilde{Q} - \tilde{Q} A^T + 2 \tilde{Q}^{1/2} [\tilde{Q}^{1/2} B U B^T \tilde{Q}^{1/2}]^{1/2} \tilde{Q}^{1/2}, \quad (3.68)$$

and $\tilde{Q})(\tau') = Q(\tau')$.

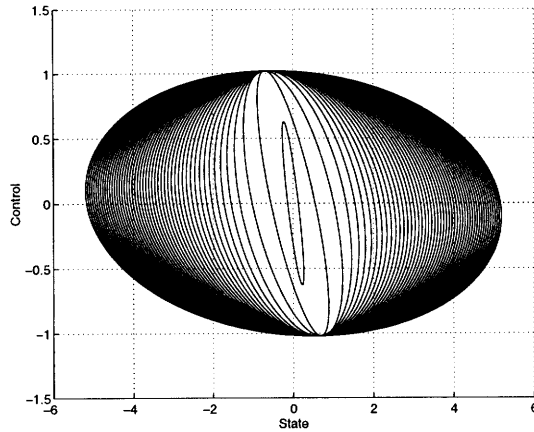


Figure 3-15: Sub-Controllable Set for State Constrained System

This is a two stage differential equation, and because of this it is no longer possible to guarantee the nesting condition at the time τ' . A set of ellipsoids generated by this method are shown in Fig. 3-15. The resulting performance for an initial condition $\mathbf{x}_0 = [5 \ 0]^T$ is shown in Fig. 3-16. We can see immediately that the performance is worse than the HPB/RC with LMI enhancements shown in Fig. 3-12 (Note that the initial condition here is half of that in Fig. 3-12). The performance is somewhat comparable with that in Fig. 3-10, but simulations showed that the time to convergence degrades much faster the further the initial condition is from the origin. This comes from the very slow growth of the sub-controllable set, which is visible in Fig. 3-15, because each ellipsoid is separated by a constant value of τ . In fact this is the major difficulty in adapting the sub-controllable set methods to state constrained systems. It is not easy to evolve the ellipsoids such that a good approximation to the actual controllable set is achieved. The problem becomes even less obvious for asymmetric systems.

3.5 Application to the F/A-18 HARV

In this section we apply the HPB (High Performance Bounded) and the HPB/RC (High Performance Bounded with Rate Constraints) methodologies developed in Sec-

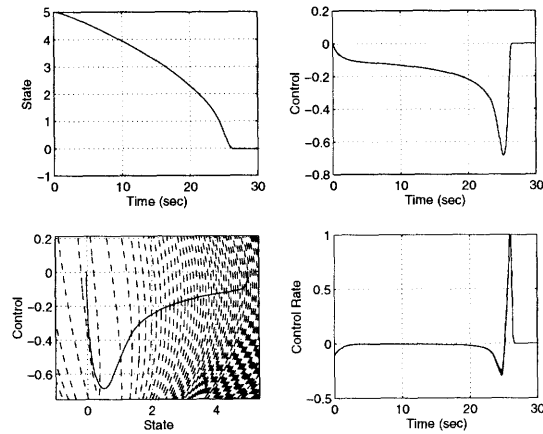


Figure 3-16: Performance for Sub-Controllable State Constrained Controller

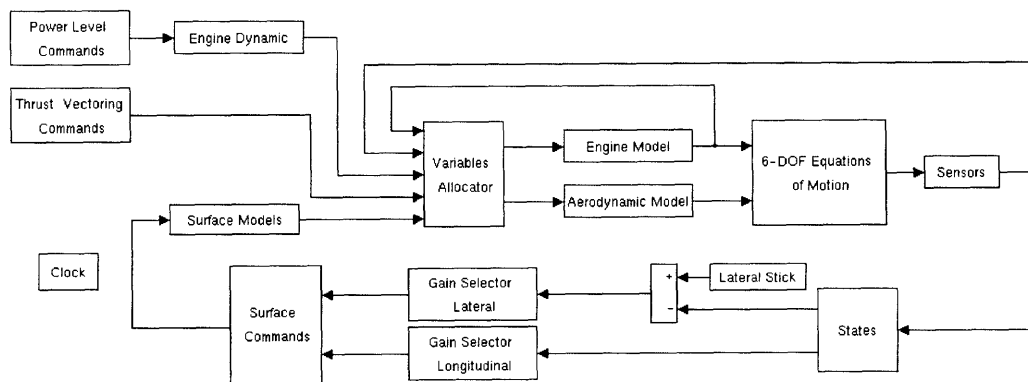


Figure 3-17: F/A-18 HARV Nonlinear Model

tion 3.1 and Section 3.3 respectively, to the lateral directional control of the F/A-18 HARV (High Alpha Research Vehicle). For this purpose a nonlinear simulator, developed by M.I.T. and NASA Dryden, of the F/A-18 HARV was used [52]. The simulator structure is pictured in Fig. 3-17 and is implemented as a SIMULINK program. The *aerodynamic model* is comprised of aerodynamic tables covering a wide range of angle of attack, mach numbers, and altitudes. At each time step 91 interpolation tables are used to calculate the contribution to the aerodynamic coefficients resulting from all the surfaces of the airplane, the flexibility terms, and the longitudinal and lateral stability derivatives. The *surface model* represents the actuators in terms of different linear models, up to fourth order, and includes rate and position saturation limits.

3.5.1 Controller Design

A single flight point design was performed for a flight condition of Mach, $M = 0.7$, and altitude, $h = 20000\text{ft}$. The linear model used for this flight condition was,

$$A_{lat} = \begin{bmatrix} -2.3142 & 0.5305 & -15.5763 & 0 \\ -0.0160 & -0.1287 & 3.0081 & 0 \\ 0.0490 & -0.9980 & -0.1703 & 0.0440 \\ 1.0000 & 0.0491 & 0 & 0 \end{bmatrix} \quad (3.69)$$

$$B_{lat} = \begin{bmatrix} 23.3987 & 21.4133 & 3.2993 \\ -0.1644 & 0.3313 & -1.9836 \\ -0.0069 & -0.0153 & 0.0380 \\ 0 & 0 & 0 \end{bmatrix} \quad (3.70)$$

The states are the, roll rate, yaw rate, sideslip, and bank angle; $x = [p \ r \ \beta \ \phi]^T$. The controls are the aileron, stabilator, and rudder; $u = [\delta_a \ \delta_s \ \delta_r]^T$. The F/A-18 HARV has symmetrical actuator rate limits and non-symmetrical position limits. However ϕ is so close to begin an integrator state that the asymmetric formulation of Section 3.2 cannot be used for this system. Thus we will only perform a design for the HPB and HPB/RC, and for each actuator the smallest of the two position bounds was selected.

The position and rate limits were chosen as

$$|\delta_a| \leq 25 \text{ deg}, \quad |\dot{\delta}_a| \leq 100 \text{ deg/s},$$

$$|\delta_s| \leq 10.5 \text{ deg}, \quad |\dot{\delta}_s| \leq 40 \text{ deg/s},$$

$$|\delta_r| \leq 30 \text{ deg}, \quad |\dot{\delta}_r| \leq 82 \text{ deg/s}.$$

The standard control law for the F/A-18 HARV longitudinal dynamics was maintained in order to keep the longitudinal states at acceptable levels. The standard HPB methodology was then used to generate a lateral directional controller to replace the standard lateral directional controller.

In general, the HPB methodology, because it is based on the LQR, is not amenable to tracking/servo problems. This can be overcome by means of an optimal tracking formulation as in [45]. However, this requires that the input be known before hand. A recent application of the LQR to an actual Flight Control System is the X-31, where the tracking problem is overcome by addition of a variable feedforward gain [7]. Indeed, the issue of tracking is an important one. In the example that follows we will avoid dealing directly with this issue by commanding only the bank angle state which acts as an integrator to achieve zero steady state error.

The controller parameters for the standard HPB were chosen as

$$r_{\max} = 6000, \quad \lambda = 1.05,$$

$$N = 150, \quad Q = \mathbf{diag}([0 \ 5 \ 7 \ 1]).$$

Finally the HPB/RC method was applied to create a controller with the parameters used in algorithm 1 as

$$r_{\max} = 1e6, \quad \lambda = 1.3, \quad N = 40,$$

$$Q_{11} = \mathbf{diag}([0 \ 5 \ 7 \ 1]), \quad \alpha = 10, \quad \beta = 10.$$

Computational times for the standard HPB are extremely quick. The HPB/RC

Controller	P.O.	3% Settling Times
STNDRD	34	3.7s
HPB	21	3.4s
HPB/RC	38	3.9s

Table 3.2: Performance for F/A-18 HARV Example

computational times are longer, with a set of 40 ellipsoids requiring 10-15 minutes to compute on a SUN SPARC 5 workstation. All three control laws (F/A-18 STNDRD,HPB,HPB/RC) were then tested for a single side turn, $\phi = 0, +90, 0$, using maximum roll rate command in the stability roll axis. When the bank angle reaches +90 the roll stick is reversed to full negative roll rate until the bank angle returns to 0. Fig. 3-18 shows the responses of the lateral states for all three controllers and Fig. 3-19 shows the control positions and rates (Dash/Dot:STNDRD Dash:HPB Solid:HPB/RC). The standard HPB provides the best response in terms of time to complete the maneuver, due to the high gains near the equilibrium that improve the settling times.

The percentage overshoot and time to settle to within 3% of the achieved bank angle are shown in Table 3.2. The sideslip and yaw rate for the HPB/RC, most likely, reach unacceptable levels. This is, in part, due to the difficulty of tuning the controller, and the limited design iterations that were performed.

It is important to note that both the HPB and HPB/RC are general design methods, where as the standard F/A-18 control law is a custom designed controller. A very pressing question in flight control law design is the benefit of such general design methods. As we have seen here it is difficult to obtain parallel or better performance with a particular general design method, let alone consider all of the multifarious aspects of a flight control system design. In fact, fixed structure methods show much promise for future control law designs [51]. The 'role' of general design methods is still difficult to place. Indeed, it is difficult to directly compare a method with guarantees to one without. These guarantees are what make such a method attractive, and possibly useful for a wide range of applications.

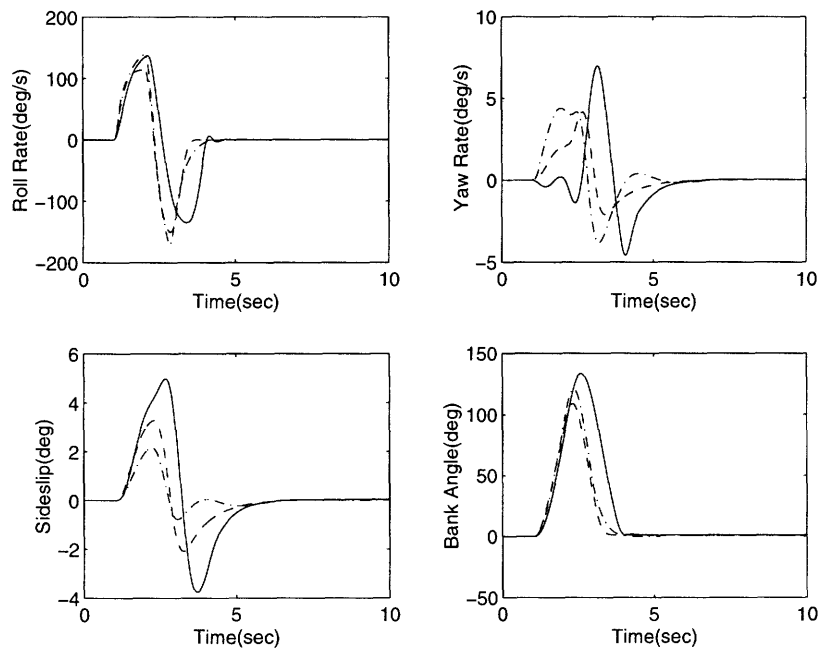


Figure 3-18: Single Side Turn Response

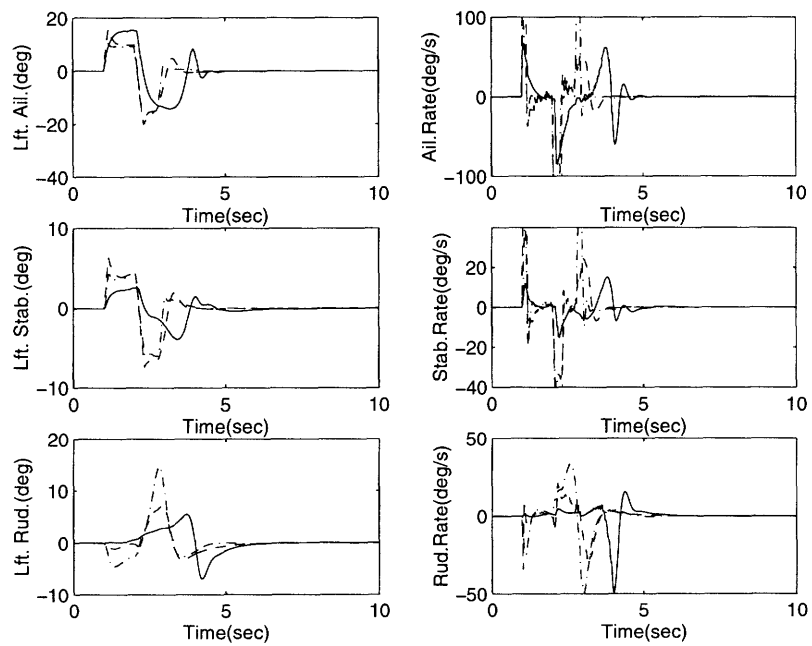


Figure 3-19: Control Surface Positions and Rates

Chapter 4

Conflict Detection and Resolution

In this chapter we will present a methodology for solving problems like the CDGC problem. The difficulty in solving the CDGC problem lies in the generality of the constraints. Quite obviously they may be non-convex sets. However, for many problems of interest, it is not unlikely that they will possess some structure. Fitting with the theme of this thesis the approach here will be one of approximation. That is, how closely can we approximate the true constraints by ones that are more amenable to convex optimization. If the constraints are non-convex then we hope for a way to formulate them as quadratics so that the QCQP can be used to obtain a lower bound on the solution. In stronger cases where the constraints can be approximated by convex functions, representable as LMIs, we will use semidefinite programming to solve the problem. To summarize, we will not present an explicit solution to the CDGC problem since it is too general to solve. Instead we will illustrate the approach through a real world problem, namely aircraft conflict detection and resolution.

The motivation and demands of the aircraft conflict detection and resolution problem are clear. Both the increasing amount of air traffic and the possibility of removing rigid airway structures in favor of Free Flight will place tremendous demands on the human air traffic controllers. It is unlikely that they will be able to handle the demands of the future without some form of automation. Safety is of critical importance both by the nature of the problem, and the commitment to increasing the safety of air travel. Thus, any automated system that detects and resolves conflicts must provide

guarantees on separation distances and computational times.

4.1 Conflict Detection

The aircraft conflict problem was discussed in the introduction. Usually a conflict is discussed in aircraft pairs. For each pair we define one aircraft as the *host* aircraft and the other as the *intruder*. It will become clear in what follows that the matter of which aircraft is the host and which is the intruder is merely one of definition. The intruder aircraft must not violate a separation parameter, which defines a radius around the host aircraft. A conflict is declared when this separation parameter is predicted to be less than a prescribed value. Obviously it is quite possible to have multiple aircraft conflicts, where several aircraft have conflicts with at least one other aircraft. A recent study has shown that six aircraft conflicts occur quite frequently under increased traffic conditions [1]. This is where the problem becomes highly combinatorial and thus complex.

Given the safety requirements of the problem we will be interested in providing *guaranteed* lower bounds on the miss distance of an aircraft pair. This characteristic is similar to the approaches in [5, 75]. Indeed, this "worst-case" approach appears to be compatible with the way Air Traffic Controllers and Pilots make decisions [2]. Consequently, this approach has a useful reachable set formulation. Given two aircraft with uncertainties in their velocities and thus positions, the detection problem is to determine if the reachable sets at some time have a non-empty intersection. That is, for each time T we desire to check if,

$$\mathcal{R}_1(T, \mathcal{X}_0) \cap \mathcal{R}_2(T, \mathcal{X}_0) = \emptyset,$$

where \mathcal{R}_1 and \mathcal{R}_2 are the reachable sets of the two aircraft that evolve according to the velocities and their uncertainties.

We will consider three two-dimensional conflict detection cases from which more complicated scenarios can be analyzed. We will take the nominal model for each

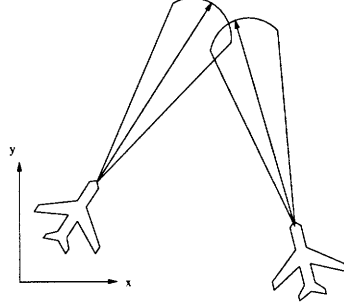


Figure 4-1: Uncertainties in the Velocities

aircraft i as

$$p_i(t) = p_{i_0} + v_{i_0}t, \quad (4.1)$$

where $p_{i_0}, v_{i_0} \in \mathbf{R}^2$ are the initial position and nominal velocity respectively. Since we will often be dealing with the relative co-ordinates of two aircraft we also define

$$p_{ij}(t) = p_j - p_i, \quad v_{ij} = v_j - v_i,$$

and,

$$p_{ij_0} = p_{j_0} - p_{i_0}, \quad v_{ij_0} = v_{j_0} - v_{i_0}.$$

The simplest form of conflict detection, for the case where the aircraft do not change course and there are no uncertainties, can be accomplished by calculating the minimum miss distance for an aircraft pair (i,j) as

$$d_{ij_0} = \begin{cases} \sqrt{\|p_{ij_0}\|^2 - \frac{(p_{ij_0}^T v_{ij_0})^2}{\|v_{ij_0}\|^2}} & \text{if } p_{ij_0}^T v_{ij_0} < 0 \\ \|p_{ij_0}\| & \text{otherwise} \end{cases} \quad (4.2)$$

However, even though uncertainties can be incorporated into this equation, it rapidly becomes difficult to use as the detection problems become more complex. Thus we attempt to propose a more flexible method based on LMI feasibility problems.

Define the perturbed version of the nominal model (4.1) for two aircraft as

$$p_i(t) = p_{i_0} + v_i t, \quad i = 1, 2. \quad (4.3)$$

where v_i is the uncertain velocity that lies in some range around the nominal. To begin with we will take uncertainties in the velocities v_{i_0} corresponding to an increasing cross track uncertainty. In other words each aircraft is allowed to drift to either side of its nominal track without any acceleration. Mathematically, the v_{i_0} must lie in the intersection of the ball

$$\|v_i - v_{i_0}\|^2 \leq \Delta_{v_i}^2, \quad i = 1, 2, \quad (4.4)$$

where Δ_{v_i} is the uncertainty, and the circle

$$\|v_i\|^2 = \|v_{i_0}\|^2, \quad i = 1, 2. \quad (4.5)$$

For each time t this describes an increasing arc of possible aircraft positions as shown in Fig. 4-1. To determine if a conflict will occur over some time interval $0 \leq t \leq t_{\max}$ we must check the condition

$$m_{\min} \geq m_0, \quad (4.6)$$

where m_{\min} is the point of closest approach and m_0 is the specified separation parameter. Using the perturbed model (4.3) this is true if and only if

$$\|p_{12}(t)\|^2 \geq m_0^2, \quad \forall t \leq t_{\max}. \quad (4.7)$$

We will now perform some manipulations to get the problem into an LMI format. In so doing, we will obtain an approximation of the reachable set that is always larger than the actual, that is, a super-reachable set. This allows us to say with certainty whether or not a collision will occur, because we are using a conservative approximation.

Substituting (4.3) into (4.7) yields,

$$\|p_{2_0} - p_{1_0} + (v_2 - v_1)t\|^2 \geq m_0^2. \quad (4.8)$$

Defining

$$z(t) = t(v_2 - v_1), \quad (4.9)$$

and substituting into (4.8) gives

$$\|p_{2_0} - p_{1_0} + z\|^2 \geq m_0^2. \quad (4.10)$$

Now note the following proven in [14].

Lemma 4.1 *The equality (4.9) is equivalent to*

$$tw^T Aw = z^T Aw$$

and

$$z^T Bz = tw^T Bz$$

where,

$$w = (v_2 - v_1)$$

for any $A, B \in \mathbf{R}^{2 \times 2}$.

The result of this lemma is to effectively convert the equality (4.9) into a quadratic relation. Now it is desired to check that (4.10) holds whenever the constraints (4.4,4.5) hold. A method for accomplishing this is by using a variant of the Lagrange multiplier technique, known as the \mathcal{S} -procedure [14]. This provides the following feasibility problem.

Feasibility Problem 4.1 *There is no collision between the aircraft pair (4.3), (i.e. $m_{\min} \geq m_0$) for $0 \leq t \leq t_{\max}$, if there exists $A, B, \lambda_i \geq 0, \gamma_i$ for $i = 1, 2$ such that*

$$\|p_{2_0} - p_{1_0} + z\|^2 - m_0^2$$

$$\begin{aligned}
& - \sum_{i=1}^2 \left\{ \lambda_i (\Delta_{v_i}^2 - \|v_i - v_{i_0}\|^2) + \gamma_i (\|v_i\|^2 - \|v_{i_0}\|^2) \right\} \\
& - 2z^T A w + 2tw^T A w - 2z^T B z + 2tw^T B z \geq 0
\end{aligned}$$

for any time $0 \leq t \leq t_{\max}$ and any v_1, v_2 . Furthermore, the above inequality is feasible for any time $0 \leq t \leq t_{\max}$ if it is feasible for $t = 0$ and $t = t_{\max}$ simultaneously.

Note that the original problem has been reduced to checking the feasibility of two LMIs in the variables $A, B, \lambda_i, \gamma_i$. Indeed, it is because of the convexity of these LMIs that we need only check the two end points of the time interval to guarantee that the LMI will also be satisfied for any time in between. The method of adjoining constraints using multipliers inherently introduces some conservatism. The amount of conservatism is often difficult to estimate, but with careful formulation it can often be made very small.

As an example, consider the problem where two aircraft are on a convergent course and it is desired to find the maximum allowable value of the bearing uncertainty. For this simulation we chose two aircraft with the following initial conditions and nominal velocities

$$\begin{aligned}
p_1 &= [0 \ 0]^T & p_2 &= [50 \ 0]^T \text{nmi} \\
v_1 &= (250/\sqrt{2})[1 \ 1]^T \text{knts} & v_2 &= (150/\sqrt{2})[-1 \ 1]^T \text{knts}.
\end{aligned} \tag{4.11}$$

The time interval to search over was chosen as $t_{\max} = 0.5\text{hrs}$, which was large enough to capture any possible collision. The radius of the protected zone was chosen as $m_0 = 5\text{nmi}$. Iterating on the bearing uncertainty yielded a lower bound of $\theta = 8.3^\circ$, where θ is the half-angle of the uncertainty envelope in Fig. 4-1. This value corresponds to the following uncertainties in velocity:

$$\begin{aligned}
\Delta_{v_1} &= 36.2\text{knts} \\
\Delta_{v_2} &= 21.7\text{knts},
\end{aligned} \tag{4.12}$$

via the simple relationship,

$$\Delta_{v_i} = \sqrt{2(\|v_{i_0}\|^2)(1 - \cos(\theta))}. \tag{4.13}$$

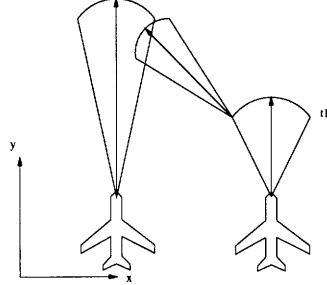


Figure 4-2: Uncertain Switch Time

In order to validate this result a Monte Carlo simulation was run with the uncertainties (4.12) as inputs to try and find the actual value of the minimum miss distance. The smallest value found was $m_{\min} = 5.01\text{nmi}$ at $t = 0.171\text{hrs}$ indicating that there is approximately 0.2% conservatism for this particular example.

The situation in Case 1 can be directly extended to the scenario when one of the aircraft may change its nominal trajectory at some unspecified time $t_1 \leq t_{\max}$. A schematic of this is shown in Fig. 4-2. It is possible that the second, or new, nominal trajectory could start at any point along the arc specified by the switch time t_1 . Additionally we will allow the new trajectory to have an uncertainty independent of the initial trajectory. The equations of the trajectories (4.3) are thus modified to include a second possible velocity for aircraft 1 as,

$$\begin{aligned} p_1(t) &= p_{1_0} + v_1^1 t_1 + v_1^2 t_2 \\ p_2(t) &= p_{2_0} + v_2^1 (t_1 + t_2) \end{aligned} \quad (4.14)$$

and we now have three uncertain velocities. As stated, the time of the switch t_1 is uncertain but after the switch occurs the new nominal covers the remainder of the time interval. Thus, we must search over the range

$$0 \leq t_1 + t_2 \leq t_{\max}, \quad (4.15)$$

to determine if a conflict is possible,

In keeping with the uncertainty model (4.4,4.5) we have

$$\begin{aligned} \|v_1^i - v_{1_0}^i\|^2 &\leq \Delta_{v_1^i}^2 & \|v_i^j\|^2 &= \|v_{i_0}^j\|^2, \quad i = 1, 2 \\ \|v_2^1 - v_{2_0}^1\|^2 &\leq \Delta_{v_2^1}^2 & \|v_2^1\|^2 &= \|v_{2_0}^1\|^2. \end{aligned} \quad (4.16)$$

Now make the definitions,

$$z_i(t) = t_i(v_2^1 - v_1^i), \quad i = 1, 2 \quad (4.17)$$

which using Lemma 4.1 are equivalent to

$$t_i w_i^T A_i w_i = z_i^T A_i w_i,$$

for any A_i , and

$$z_i^T B z_i = t_i w_i^T B_i z_i,$$

for any B_i , where,

$$w_i = (v_2^1 - v_1^i).$$

Once again we use the \mathcal{S} -procedure to arrive at the following feasibility problem.

Feasibility Problem 4.2 *There is no collision between the aircraft pair (4.3), (i.e. $m_{\min} \geq m_0$) for $0 \leq t \leq t_{\max}$, if there exists $A_i, B_i, i = 1, 2; \lambda_i \geq 0, \gamma_i$ for $i = 1, \dots, 3$ such that*

$$\begin{aligned} &\|p_{2_0} - p_{1_0} + z_1 + z_2\|^2 - m_0^2 \\ &- \sum_{i=1}^2 \left\{ \lambda_i (\Delta_{v_1^i}^2 - \|v_1^i - v_{1_0}^i\|^2) + \gamma_i (\|v_1^i\|^2 - \|v_{1_0}^i\|^2) \right\} \\ &- \lambda_3 \left\{ \Delta_{v_2^1}^2 - \|v_2^1 - v_{2_0}^1\|^2 \right\} + \gamma_3 (\|v_2^1\|^2 - \|v_{2_0}^1\|^2) \\ &\sum_{i=1}^2 -2z_i^T A_i w_i + 2t_i w_i^T A_i w_i - 2z_i^T B_i z_i + 2t_i w_i^T B_i z_i \geq 0 \end{aligned}$$

for any time $0 \leq t \leq t_{\max}$ and any v_1^1, v_1^2, v_1^3 . Furthermore, the above inequality is feasible for any time $0 \leq t_1 + t_2 \leq t_{\max}$ if it is feasible for $(t_1, t_2) \in \{(0, 0), (0, t_{\max}), (t_{\max}, 0)\}$

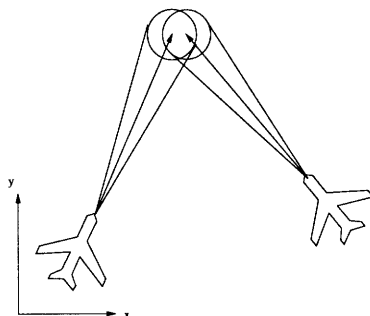


Figure 4-3: Uncertain Acceleration

As an example, let us take the case where two aircraft are initially on a parallel course 100 nmi apart with one aircraft proceeding slightly faster:

$$\begin{aligned} p_1 &= [100 \ 0]^T \text{nmi} & p_2 &= [0 \ 0]^T \\ v_1^1 &= [0 \ 240]^T \text{knts} & v_2^1 &= [0 \ 200]^T \text{knts}. \end{aligned} \quad (4.18)$$

At some point in a 1hr time interval the first aircraft makes a heading change and decreases speed such that a conflict may become a possibility, that is,

$$v_1^2 = [-40 \ 120]^T \text{knts}.$$

Given that there is a 5° uncertainty in the bearings of the two aircraft it is desired to find the closest distance of approach. Iterating on the LMI feasibility problem given above, a lower bound on the minimum miss distance was $m_{\min}=40\text{nmi}$. The result of a corresponding Monte Carlo simulation after 500000 iterations was 51nmi. This would seem to indicate a conservatism of approximately 22% for this example. However, due to the additional complexity of this problem it is hard to determine how accurate the results of the Monte Carlo simulation are.

In the next case we allow for both cross-track and along-track fluctuations, that is, in addition to the velocity uncertainties (4.4,4.5) both aircraft will also be allowed to accelerate. Geometrically this leads to a situation where the trajectory at any

time t lies on the intersection of an arc and a ball. For illustration purposes Fig. 4-3 represents the situation where only acceleration uncertainties exist. The perturbed equations of motion must be modified to include an acceleration term as

$$p_i(t) = p_{i_0} + v_i t + a_i t^2/2, \quad i = 1, 2. \quad (4.19)$$

where a_i is allowed acceleration. We allow for the previous velocity uncertainties (4.4,4.5) and the uncertainty in acceleration as

$$\|a_i\|^2 \leq \Delta_{a_i}^2, \quad i = 1, 2.$$

Define

$$z = \begin{bmatrix} z_1 \\ z_2 \end{bmatrix} = t \begin{bmatrix} (a_2 - a_1)/2 \\ v_2 - v_1 + z_1 \end{bmatrix}. \quad (4.20)$$

Which is equivalent to

$$tw^T Aw = z^T Aw,$$

for any A , and

$$z^T Bz = tw^T Bz,$$

for any B , where,

$$w = \begin{bmatrix} (a_2 - a_1)/2 \\ v_2 - v_1 + z_1 \end{bmatrix}. \quad (4.21)$$

Feasibility Problem 4.3 *There is no collision between the aircraft pair (4.19), (i.e. $m_{\min} \geq m_0$) for $0 \leq t \leq t_{\max}$, if there exists $A, B, \lambda_i \geq 0$ for $i = 1, \dots, 4$ and γ_i for $i = 1, 2$ such that*

$$\begin{aligned} & \|p_{2_0} - p_{1_0} + z_2\|^2 - m_0^2 \\ & - \sum_{i=1}^2 \left\{ \lambda_i (\Delta_{v_i}^2 - \|v_i - v_{i_0}\|^2) + \gamma_i (\|v_i\|^2 - \|v_{i_0}\|^2) \right\} \\ & - \sum_{i=1}^2 \lambda_{i+2} (\Delta_{a_i}^2 - \|a_i\|^2) \\ & - 2z^T Aw + 2tw^T Aw - 2z^T Bz + 2tw^T Bz \geq 0 \end{aligned}$$

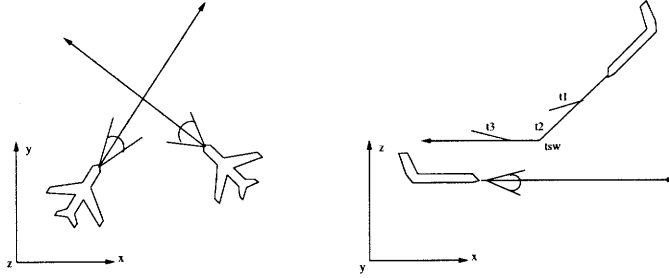


Figure 4-4: 3-Dimensional Case

for any time $0 \leq t \leq t_{\max}$ and any v_1, v_2, a_1, a_2 . Furthermore, the above inequality is feasible for any time $0 \leq t \leq t_{\max}$ if it is feasible for $t = 0$ and $t = t_{\max}$ simultaneously.

In this example consider the situation where one aircraft is flying on a course perpendicular to the other:

$$\begin{aligned} p_1 &= [0 \ 0]^T & p_2 &= [150 \ 125]^T \text{nmi} \\ v_1 &= [0 \ 250]^T \text{knts} & v_2 &= [-250 \ 0]^T \text{knts}. \end{aligned} \tag{4.22}$$

Given that the uncertainty in the acceleration of each aircraft is

$$\Delta_{a_1} = \Delta_{a_2} = 15 \text{nmi/s}^2$$

the task is to determine what the minimum miss distance will be. For the purposes of this example, only acceleration uncertainties were allowed, i.e. $\Delta_{v_i} = 0$. Iterations based on the LMI feasibility problem yielded a value for the lower bound on the miss distance of $m_{\min} = 13.2 \text{nmi}$. The result of the corresponding Monte Carlo simulation was $m_{\min} = 13.3 \text{nmi}$, indicating a conservatism of about .8%.

4.2 3-Dimensional Case

The three cases described above provide a basic set from which a wide range of problems can then be formulated and solved. Here we will present a scenario where

motion in all three dimensions must be taken into account. Consider the problem shown in Fig. 4-4 where one aircraft is on a straight and level flight path. The second aircraft is descending into a possible conflict and is told to by the ATC to make a change in its descent rate at some time $t = t_{sw}$. Now, given that the descending aircraft can make a descent rate change some time before or after t_{sw} , and that there is some possible delay in the switch Δt_{sw} , it is desired to determine whether a conflict will occur. This is a well known situation for which TCAS encounters difficulty [2]. Following the methodology described above the equations of motion for this case can be formulated as

$$\begin{aligned}
 p_1(t) &= p_{1_0} + v_1^1(t_1 + t_2 + t_3) \\
 h_1(t) &= h_{1_0} + u_1^1 t_1 + u_1^2 t_2 + u_1^3 t_3 \\
 p_2(t) &= p_{2_0} + v_2^1(t_1 + t_2 + t_3) \\
 h_2(t) &= h_{2_0} + u_2^1(t_1 + t_2 + t_3),
 \end{aligned} \tag{4.23}$$

where the h_i and u_i^j represent the vertical positions and velocities. The uncertainties in the horizontal velocities will be represented as (4.4,4.4). The vertical velocity uncertainties will simply be allowed to range over some interval

$$(u_1^i - u_{1_0}^i)^2 \leq \Delta_{u_1^i}^2, \quad i = 1, \dots, 3,$$

$$(u_2^1 - u_{2_0}^1)^2 \leq \Delta_{u_2^1}^2.$$

The protected airspace will be represented as a cylinder in the z axis [30]. This miss distance constraint can be described in the LMI format by saying that, $\forall t \leq t_{\max}$

$$\|p_{12}(t)\|^2 \geq (m_0^{xy})^2,$$

holds whenever

$$(h_2(t) - h_1(t))^2 \leq (m_0^z)^2,$$

where m_0^{xy} and m_0^z are the radius of the protected zone in the $x - y$ plane and the height of the cylinder respectively. We make the following definitions,

$$z_i(t) = \begin{bmatrix} z_{1i} \\ z_{2i} \end{bmatrix} = t_i \begin{bmatrix} v_2^1 - v_1^1 \\ u_2^1 - u_1^1 \end{bmatrix}, \quad i = 1, \dots, 3, \quad (4.24)$$

which are equivalent to

$$t_i w_i^T A_i w_i = z_i^T A_i w_i,$$

for any A_i , and

$$z_i^T B z_i = t_i w_i^T B_i z_i,$$

for any B_i , where,

$$w_i(t) = \begin{bmatrix} v_2^1 - v_1^1 \\ u_2^1 - u_1^1 \end{bmatrix}, \quad i = 1, \dots, 3. \quad (4.25)$$

At this point it is useful to observe that the problem can be broken into two phases. The first phase being before the determined switch t_{sw} , which is accompanied by one uncertain switch, and the second phase being the time after the switch, which is also accompanied by one uncertain switch. This leads to the following two "time regions"

$$0 \leq t_1 + t_2 \leq t_{sw} + \Delta t_{sw}, \quad \text{with } t_3 = 0, \quad (4.26)$$

and

$$t_{sw} \leq t_1 + t_2 \leq t_{sw} + \Delta t_{sw}, \quad \text{with } 0 \leq t_1 + t_2 + t_3 \leq t_{\max}. \quad (4.27)$$

Essentially this requires us to first check three LMIs for phase one and eight LMIs for phase two in order to solve this problem. This is summarized in the following.

Feasibility Problem 4.4 *There is no collision (ie. $m_{\min} \geq m_0$), for $0 \leq t \leq t_{\max}$, if there exists A_i, B_i for $i = 1, \dots, 3$, $\lambda_i \geq 0$ for $i = 1, \dots, 7$ and γ_i for $i = 1, 2$ such that*

$$\begin{aligned} & \|p_{20} - p_{10} + z_{11} + z_{12} + z_{13}\|^2 - (m_0^{xy})^2 \\ & - \lambda_1 \left\{ (m_0^z)^2 - \|h_{20} - h_{10} + z_{21} + z_{22} + z_{23}\|^2 \right\} \end{aligned}$$

$$\begin{aligned}
& - \sum_{i=1}^2 \left\{ \lambda_{i+1} (\Delta_{v_i^1}^2 - \|v_i^1 - v_{i_0}^1\|^2) + \gamma_i (\|v_i^1\|^2 - \|v_{i_0}^1\|^2) \right\} \\
& - \sum_{i=1}^3 \lambda_{i+3} (\Delta_{u_i^1}^2 - \|u_i^1 - u_{i_0}^1\|^2) - \lambda_7 (\Delta_{u_2^1}^2 - \|u_2^1 - u_{2_0}^1\|^2) \\
& \sum_{i=1}^3 -2z_i^T A_i w_i + 2t_i w_i^T A_i w_i - 2z_i^T B_i z_i + 2t_i w_i^T B_i z_i \geq 0
\end{aligned}$$

for any times for any times t_1, t_2 and t_3 subject to (4.26) and (4.27) and any $v_1^1, v_2^1, u_1^1, u_2^1, u_3^1, u_2^1$. Furthermore, the above inequality is feasible for any times t_1, t_2 and t_3 subject to (4.26) and (4.27) if it is feasible for $(t_1, t_2, t_3) \in \{(0, 0, 0), (0, t_{\max}, 0), (t_{\max}, 0, 0)\}$ (phase 1) and for $(t_1, t_2, t_3) \in \{(t_{sw}, 0, 0), (t_{sw} + \Delta t_{sw}, 0, 0), (0, t_{sw}, 0), (0, t_{sw} + \Delta t_{sw}, 0), (t_{sw}, 0, t_{\max} - t_{sw}), (t_{sw} + \Delta t_{sw}, 0, t_{\max} - t_{sw} - \Delta t_{sw}), (0, t_{sw}, t_{\max} - t_{sw}), (0, t_{sw} + \Delta t_{sw}, t_{\max} - t_{sw} - \Delta t_{sw})\}$ (phase 2).

Consider a straightforward example of the above where the aircraft motion is confined to the $x - z$ plane. The two aircraft are given the initial positions

$$\begin{aligned}
p_1 &= [4 \ 0]^T & p_2 &= [-3 \ 0]^T \\
h_1 &= 2.5 & h_2 &= 0,
\end{aligned} \tag{4.28}$$

where the units have been dropped for convenience. The first aircraft is on a descent that could cause a conflict with the second aircraft which is on a straight and level course. The first aircraft is told to level out at $t_{sw} = 3$. There is a possible delay $\Delta t_{sw} = .1$ and the first aircraft is allowed an uncertain change in its nominal vertical velocity after t_{sw} . The problem is searched over the time interval $t_{\max} = 10$. The nominal velocities were set as

$$\begin{aligned}
v_1^1 &= [-1 \ 0]^T & v_2^1 &= [1 \ 0]^T \\
u_1^1 &= -.5, \ u_2^1 = 0, \ u_3^1 = -.2 & u_2^1 &= 0
\end{aligned} \tag{4.29}$$

Given that there is a 5° horizontal bearing uncertainty in each aircraft it is desired to find the maximum allowable uncertainty in the vertical velocity given that the

protected cylinder has its parameters set as,

$$m_0^{xy} = 0.5, m_0^z = 0.1.$$

Iterating on the vertical velocity uncertainty yielded a lower bound $\Delta_{v_1^3} = 0.1$. Several attempts at using Monte Carlo methods to validate this result were made, but it was difficult to obtain a consistent result with any level of confidence. Thus at this time it is difficult to estimate the conservatism associated with the result of this example. Indeed, in general, the Monte Carlo simulations worked well only for the more simple cases with few variables and small uncertainty levels.

4.3 Conflict Resolution

Once the detection stage has been completed each aircraft involved in the conflict must be issued a resolving command. We will need to make some simplifying assumptions in the approach to be given, and these are as the follows.

1. All aircraft travel in straight lines.
2. There is no uncertainty in position or
3. All motion occurs only in the horizontal plane
4. All aircraft turns occur instantaneously without loss of speed, etc.
5. All aircraft co-operate in resolving conflicts

The validity of each of these assumptions requires some discussion. Assumption 1 is not that limiting since aircraft would always prefer to fly straight and level at all times. That is, we expect each aircraft to be on a straight and level flight path before the conflict resolution begins. Assumption 2 seems unrealistic, but it is possible to absorb uncertainties in aircraft trajectories into the separation parameters. Assumption 3 is only limiting in that we choose not to resolve conflicts by climbing or descending. In other words, it is a limitation of our algorithm, not of the model.

Assumption 4 is an approximation the validity of which has been discussed in [5, 18]. In practice we expect there to be some delay in the time it takes for an aircraft to acquire a new heading. However, this can be overcome by a continual update of the resolution command, or the addition of margins to the separation parameters. Furthermore, we will impose constraints in the resolution algorithm that will limit the range of velocities that can be commanded. Finally, Assumption 5 is quite reasonable for commercial aircraft, since they will all be equipped with the same electronics and working under the guidance of an traffic controller.

Given these assumptions, we will use the nominal model (4.1). Now with the change in focus we re-define the vector v_{i_0} to be the desired velocity, *i.e.* the velocity vector that each aircraft would like to have. The vector v_i now becomes the decision or control input and this is what we desire to compute. We have already seen that the closest point of approach between any aircraft pairing (i, j) is given by (4.2). Thus, it is logical that we should start with trying to build a conflict resolution algorithm around the constraint

$$\|p_{ij_0}\|^2 - \frac{(p_{ij_0}^T v_{ij})^2}{\|v_{ij}\|^2} \geq d_{ij}^2, \quad (4.30)$$

where d_{ij} is the separation parameter, and v_{ij} is the decision or control variable. Unfortunately this constraint is not convex. Fig. 4-5 shows two aircraft engaged in a conflict in relative co-ordinates. The region marked with solid lines specifies all the v_{ij} for which a conflict will occur. The unmarked, or admissible region, is specified by the constraint (4.30). Aside from not being convex the constraint (4.30) also has another important feature. This is the fact that it will not allow for conflicts in the past. That is, the trajectories of two aircraft that are heading away from each other will not necessarily satisfy (4.30) and this is reflected by the region marked with dashed lines. This does not pose a serious problem for two reasons. First, the detection stage is used to determine the possible conflicts, thus aircraft whose trajectories have past conflicts will be removed from the resolution problem. Secondly, we will show how this can also be removed by an alternate formulation.

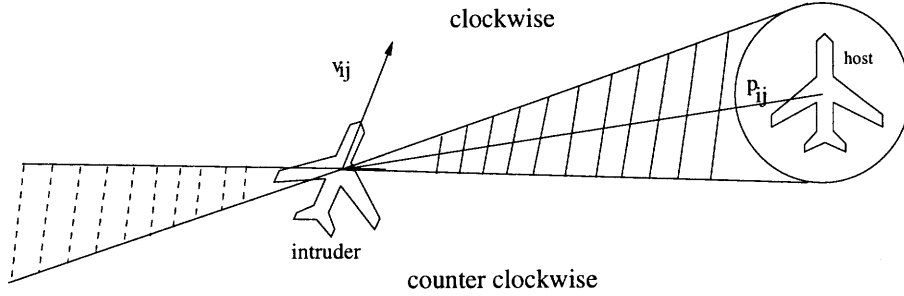


Figure 4-5: Relative Motion and Admissible Regions

Regardless, the admissible region can be observed to represent two connected convex regions (connected at the center of the intruder aircraft). Physically these correspond to the two possible crossing patterns for any aircraft pair. These are the cases when the aircraft cross each other *clockwise* (each pilot sees the other drift from left to right), or *counter clockwise* (each pilot sees the other aircraft drift from right to left). Thus, our first attempt will be to formulate the convex constraints corresponding to these two admissible regions.

The inequality (4.30) can be converted to a more convenient form by means of the standard vector identity

$$(a \times b)^2 = |a|^2|b|^2 - (a^T b)^2$$

to obtain

$$v_{ij}^T \left(\frac{d_{ij}^2 I}{|\gamma|} \right) v_{ij} \leq |\gamma|, \quad (4.31)$$

where

$$\gamma = \det \begin{bmatrix} p_{ij}^T \\ v_{ij}^T \end{bmatrix}, \quad (4.32)$$

and the sign of γ represents the crossing direction, positive for counter-clockwise (CCW) and negative for clockwise (CW). We can now use Schur complements to

write this as an LMI. Assume $\gamma > 0$, then we can write

$$\begin{bmatrix} \gamma/d_{ij}^2 & v_{ij}^T \\ v_{ij} & \gamma I \end{bmatrix} > 0. \quad (4.33)$$

Thus, using the constraint (4.33) in a resolution algorithm would always force the ij th pairing to cross CCW, corresponding to the lower cone in Fig. 4-5. Likewise we can write the LMI for the opposite direction by simply changing the sign of the LMI.

The problem of allowing for conflicts that happened in the past can be remedied by writing (4.30) as two linear constraints. Indeed, defining the angle between v_{ij} and $-p_{ij}$ to be θ , (4.30) reduces to

$$\cos \theta \leq \sqrt{1 - \frac{d_{ij}^2}{|p_{ij}|^2}} \text{ and } \sin \theta \geq \sqrt{\frac{d_{ij}^2}{|p_{ij}|^2}}, \quad (4.34)$$

where $\theta \in [-\pi/2 \pi/2]$. Thus we arrive at the two half spaces,

$$\mu_{CCW}^T v_{ij} \geq 0 \quad (4.35)$$

and

$$\mu_{CW}^T v_{ij} \geq 0, \quad (4.36)$$

where

$$\mu_{CCW} = \Gamma p_{ij}, \quad \mu_{CW} = \Gamma^{-1} p_{ij},$$

and

$$\Gamma = \begin{bmatrix} \sqrt{\frac{d_{ij}^2}{|p_{ij}|^2}} & -\sqrt{1 - \frac{d_{ij}^2}{|p_{ij}|^2}} \\ \sqrt{1 - \frac{d_{ij}^2}{|p_{ij}|^2}} & \sqrt{\frac{d_{ij}^2}{|p_{ij}|^2}} \end{bmatrix}. \quad (4.37)$$

The two constraints (4.35,4.36) independently represent the CW and CCW solutions. Thus the admissible region is now defined by two half-spaces. Clearly, these constraints are also LMIs, but they also suggest a possible Linear Programming formulation that we will neglect to discuss here.

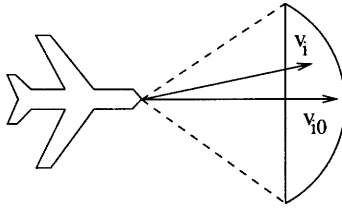


Figure 4-6: Constraints on Aircraft Velocities

The next step is to formulate the constraints on the decision vector v_i . As stated in the assumptions we desire the aircraft to travel at constant velocities. In keeping with the turning model we must impose constraints on the allowable velocity range. However, the constant velocity constraint

$$v_i^T v_i = v_{i0}^T v_{i0}$$

is nonconvex. Once again we are left with the problem of approximation. A simple and practical solution, that limits the velocity and the turning radius is pictured in Fig. 4-6. That is, we will bound the decision vector by a half-moon shape specified by the following constraints:

$$\begin{aligned} v_i^T v_i &\leq v_{i0}^T v_{i0} \\ \alpha v_{i0}^T v_{i0} &\leq v_i^T v_{i0}, \end{aligned} \tag{4.38}$$

where the parameter α specifies both the allowable decrease in velocity and the maximum heading change

$$\theta_{\max} = \arccos(\alpha).$$

For example, allowing for a 10% speed variation, $\alpha = .9$, gives $\theta_{\max} = 25.8^\circ$. The assumption of a 10% speed variation is quite valid in practice for both the Boeing 727 and McDonnell Douglas MD-11.

To complete the resolution algorithm we require an objective function. Indeed, a simple objective that is linear and makes good practical sense is to maximize the projection of the decision vector on to the nominal velocity vector. Thus given n

aircraft we have the following conflict resolution algorithm, formulated as a convex optimization problem.

$$\begin{aligned}
& \text{maximize} && \sum_{i=1}^n v_i^T v_{i_0} \\
& \text{subject to} && \text{one of (4.35), (4.36) for each pair } ij \text{ and (4.38)} \\
& && i = 1, \dots, n-1, j = i+1, \dots, n
\end{aligned} \tag{4.39}$$

The choice of which constraints, (4.35) or (4.36), to use must be decided upon before hand. Clearly, unless we have some knowledge that suggests what crossing patterns to use we must check $2^{\frac{n(n-1)}{2}}$ permutations. Obviously, this is prohibitive for more than four aircraft ($n = 5$ implies 1024 permutations). What we really need is some way to reduce the complexity of the problem. As we have seen, the problem of choosing between the possible crossing patterns is nonconvex. However, using the knowledge of Chapter 2 we know that we may compute a lower bound by formulating the problem as a QCQP and solving the dual optimization problem.

4.4 Computation of the Lower Bound

Notice that the constraints (4.30,4.38) and the objective in (4.39) can all be represented as quadratic functions in the variables v_i . We can use the constraints (4.30,4.38) on the basis that past conflicts can be removed by means of a detection algorithm. Thus, this implies the conflict resolution with non-directional constraint (4.30) can be formulated as a QCQP. From this, as we described in Section 2.1.2, a lower bound can be computed by solving the problem (2.17).

Let, $x = [v_1^T v_2^T \dots v_n^T]^T$ be the variable. We can then formulate the $P(\lambda), q(\lambda)$, and $r(\lambda)$ as follows. The objective appears as

$$\begin{aligned}
P_0 &= 0 \\
q_0 &= -\frac{1}{2}[v_{1_0}^T v_{2_0}^T \dots v_{n_0}^T]^T \cdot \\
r_0 &= 0
\end{aligned} \tag{4.40}$$

We can then formulate the $n(n-1)/2$ matrices that correspond to (4.30) as

$$\begin{aligned}
P_{j+(i-1)n-i(i+1)/2}(l, m) &= \begin{bmatrix} (d_{ij}^2 - p_{ij}^T p_{ij})I + p_{ij} p_{ij}^T & -(d_{ij}^2 - p_{ij}^T p_{ij})I - p_{ij} p_{ij}^T \\ -(d_{ij}^2 - p_{ij}^T p_{ij})I - p_{ij} p_{ij}^T & (d_{ij}^2 - p_{ij}^T p_{ij})I + p_{ij} p_{ij}^T \end{bmatrix} \\
q_{j+(i-1)n-i(i+1)/2} &= 0 \\
r_{j+(i-1)n-i(i+1)/2} &= 0, \quad i = 1, \dots, n-1, \quad j = i+1, \dots, n,
\end{aligned} \tag{4.41}$$

where $l = \{i, i+1, j, j+1\}$, $m = \{i, i+1, j, j+1\}$, and any un-assigned elements are zero. Next are the $2n$ velocity constraint matrices (4.38) formulated as

$$\begin{aligned}
P_{n(n-1)/2+1+i}(\{i, i+1\}, \{i, i+1\}) &= I \\
q_{n(n-1)/2+1+i} &= 0 \\
r_{n(n-1)/2+1+i} &= -v_{i_0}^T v_{i_0}, \quad i = 1, \dots, n,
\end{aligned} \tag{4.42}$$

and

$$\begin{aligned}
P_{n(n-1)/2+1+n+i} &= 0 \\
q_{n(n-1)/2+1+n+i}(\{i, i+1\}, \{1, 2\}) &= -\frac{1}{2}v_{i_0} \\
r_{n(n-1)/2+1+n+i} &= \alpha v_{i_0}^T v_{i_0}, \quad i = 1, \dots, n.
\end{aligned} \tag{4.43}$$

As stated, solving the problem (2.17) provides a lower bound, $\gamma^* \leq J_{OPT}^*$, where γ^* is the optimal obtained from the solution to (2.17) and J_{OPT}^* is the optimal value obtained from the minimum of all the possible permutations. Without saying anything further we can immediately see a possible savings in computation time. As we search through the permutations we will have a gauge of how close we are to the optimal. Indeed, if $\gamma^* = J_{OPT}^*$, then we will know that the optimal has been achieved. However, the worst case is still $2^{n(n-1)/2}$. What we really desire is for the lower bound to somehow always provide a solution, thus, reducing the problem to the solution of only one convex optimization problem. This may not be possible but some recent research has shown promise. In [13] the authors showed that computation of the lower bound stability margin of the Popov criterion can be used to compute a good upper bound by looking into the null space of the constraint matrix at the optimal. In the spirit of this result, we now assert the following.

Lemma 4.2 Assume $\gamma^* = J_{OPT}^*$ and there exists a dual optimal λ^* and primal optimal x^* . Then there exists a vector $v^* = [x^{*T} \ 1]^T$ that is a null eigenvector of the matrix

$$\begin{bmatrix} -P(\lambda^*) & q(\lambda^*) \\ q(\lambda^*)^T & \gamma - r(\lambda^*) \end{bmatrix} \quad (4.44)$$

Proof: By virtue of the fact that strong duality holds, we have,

$$\begin{aligned} x^{*T} P_0 x^* + 2q_0^T x^* + r_0 &\leq x^{*T} P_0 x^* + 2q_0^T x^* + r_0 \\ &+ \sum_{i=1}^n \lambda_i^* (x^{*T} P_i x^* + 2q_i^T x^* + r_i) \end{aligned} \quad (4.45)$$

and thus,

$$\sum_{i=1}^n \lambda_i^* (x^{*T} P_i x^* + 2q_i^T x^* + r_i) \geq 0.$$

Since λ^* is dual feasible, $\lambda^* \geq 0$ and x^* is primal feasible we have

$$\sum_{i=1}^n \lambda_i^* (x^{*T} P_i x^* + 2q_i^T x^* + r_i) \leq 0.$$

Thus,

$$\sum_{i=1}^n \lambda_i^* (x^{*T} P_i x^* + 2q_i^T x^* + r_i) = 0.$$

Now because of strong duality we also have,

$$x^{*T} P_0 x^* + 2q_0^T x^* + r_0 = \gamma^*.$$

and further,

$$x^{*T} P_0 x^* + 2q_0^T x^* + r_0 + \sum_{i=1}^n \lambda_i^* (x^{*T} P_i x^* + 2q_i^T x^* + r_i) = \gamma^*.$$

and

$$\begin{bmatrix} x^* \\ 1 \end{bmatrix}^T \begin{bmatrix} P(\lambda^*) & q(\lambda^*) \\ q(\lambda^*)^T & r(\lambda^*) - \gamma \end{bmatrix} \begin{bmatrix} x^* \\ 1 \end{bmatrix} = 0 \quad (4.46)$$

and thus, by a simple manipulation, v^* is a null eigenvector for (4.44). ■

Thus we can infer that when the lower bound is tight there will exist a null eigenvector that is the solution to the original problem. This also implies that if the null eigenvector is unique than the lower bound is a tight one [13]. For our problem the following question quickly arises. How often is the bound tight? Or the somewhat equivalent question, how often is there only one null eigenvector, and when there is does it yield the optimal solution? It is difficult to obtain precise answers to these questions. Indeed, we must rely on some statistical analysis at this point to provide enlightenment. In the following we will give an example of some of the statistical techniques that could be used to provide a better understanding of the lower bound.

Given there are n aircraft, the solution matrix has exactly $2n + 1$ eigenvalues. Let ρ_i be the i th eigenvalue of the matrix

$$\begin{bmatrix} -P(\lambda^*) & q(\lambda^*) \\ q(\lambda^*)^T & \gamma - r(\lambda^*) \end{bmatrix}, \quad (4.47)$$

where λ^* is the value of λ at the best lower bound obtainable. Define the following function,

$$\gamma(\delta) = \sum_i^{n(n-1)/2} (|\rho_i| \leq \delta)$$

which is a measure of the number of eigenvalues below a certain value δ . This function cannot be exactly computed, but we can approximate it via statistical methods. For example, Fig. 4-7 shows a plot of

$$\frac{\text{\#of times } \gamma(\delta) = 1}{N},$$

where $N = 1000$ is the number of trials, for the case of 2,4, and 8 aircraft. The data was created by generating aircraft trajectories with the random distribution

$$\begin{aligned} |(p_{ij_0})_k| &\leq 5, \\ |(v_{ij_0})_k| &\leq 2, \quad k = 1, \dots, 2, \end{aligned} \quad (4.48)$$

where $(\cdot)_k$ is the k th element. The separation parameter and speed variation were

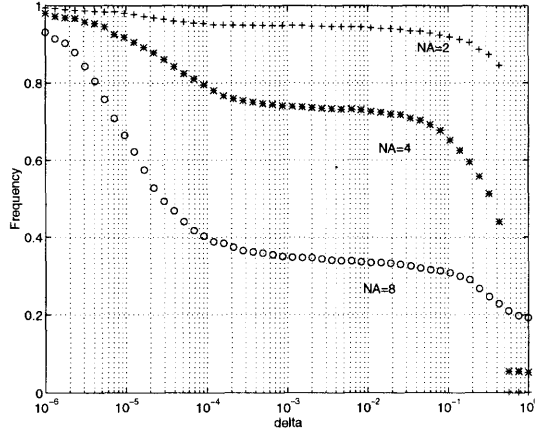


Figure 4-7: Frequency of Null Eigenvector

chosen as

$$d_{ij} = 1, \text{ and } \alpha = .9.$$

All simulations were performed with the software package [24], which is a front end parser for [77]. As should be expected the frequency of the null eigenvector decreases as δ increases. Logically we would like to know for each value of δ what percentage of the cases does the null eigenvector provide the optimal solution.

In answer to this question we must again use some form of statistical method. For example, a set of 100 trials with four aircraft was generated with the same simulation parameters above. An example of one of these four aircraft conflicts is shown in Fig. 4-8. The actual minimum was found by computing each of the 64 permutations. Table 4.1 shows, for each value of δ the percentage of times that the function $\gamma = 1$, and what percentage that null eigenvector yielded the optimal solution. Thus we can see that as the level of δ is decreased we have less of a chance of extracting the optimal. This makes perfect sense, since the lower the value of δ the more likely there is another eigenvalue close to zero that has not been taken into account.

What then can be said about cases where more than one null eigenvector exists. Consider the case where there are two null eigenvectors, $v_1 = [x_1^T \ t_1]^T$ and $v_2 = [x_2^T \ t_2]^T$, where $x_i \in \mathbf{R}^{2n}$, and the v_i correspond to eigenvalues below a certain value δ . A reasonable place to start is to look at the linear combination of v_1 and v_2 . As

δ	$\gamma = 1 \%$	Exact Solution%
1e-3	66	100
1e-4	74	88
1e-5	83	80

Table 4.1: Null Eigenvector Solution Percentages

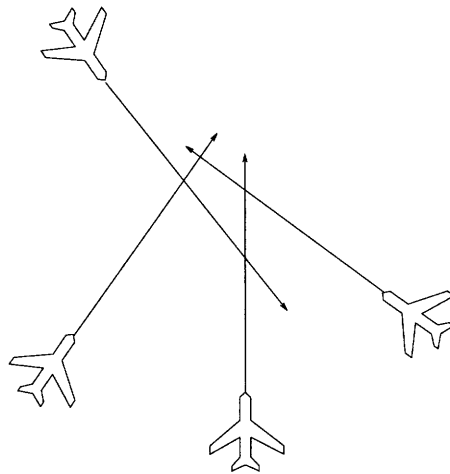


Figure 4-8: Example of a 4 Aircraft Conflict

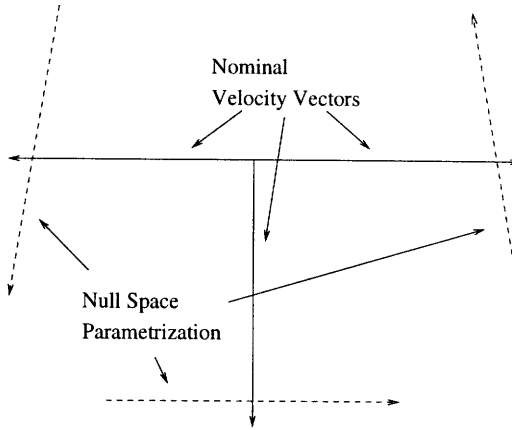


Figure 4-9: Null Space Parameterization

we know from the formulation of the QCQP we require that $t_1 + t_2 = 1$ in order for the linear combination to be a possible solution. Thus we can parameterize the combination as

$$\hat{v} = \begin{bmatrix} x_1 \\ 1 - t_1 \end{bmatrix} + \begin{bmatrix} x_2 \\ t_2 \end{bmatrix}, \quad (4.49)$$

where t_2 is allowed to range over some interval. A schematic of this is shown in Fig. 4-9 for a three aircraft symmetrical case. What we hope for is that the parameterization somehow indicates where the optimal solution lies. For example, for each value of t_2 we could look at the crossing direction that is implied, by computing (4.32) for each aircraft pair. This could then be input into the algorithm (4.39) to determine if it is feasible. This process would have to be continued in a line search manner to find a solution. Fig. 4-9 which is based on an actual test case indicates that the solution is either all CW or all CCW by noting the direction of the arrows. Indeed these are the two optimal solutions for this case.

These types of analysis methods based on the lower bound require a much further investigation than what is given here. We have simply attempted to provide an overview of some of the techniques that might be employed to reduce the complexity of the original problem.

Chapter 5

Conclusions and Recommendations

The goal of this thesis has been to provide two practically useful methodologies for two very significant constrained control problems. Underlying this was the need to provide guaranteed solution methods that are computationally efficient with good performance.

5.1 Nonlinear Control for Nonlinear Actuators

The first problem was the control of Linear Time Invariant systems subject to nonlinear actuators. Three different nonlinear actuator problems were considered. In summary these are systems subject to actuator position constraints, systems subject to asymmetric actuator position constraints, and systems subject to actuator position and rate constraints. The methodology developed was a nonlinear state feedback control scheduled according to the state to avoid saturation at all times. This is accomplished by using a set of nested invariant ellipsoids, that for each value of the nonlinear gain, approximate the maximal invariant region. By construction, the method provides guaranteed control boundedness and stability. Several simple examples were given to demonstrate the methods along with a comparison to sub-controllable sets and a more significant application to a nonlinear simulator of the

F/A-18 HARV. Through out all of this, computational efficiency was obtained because everything was formulated as a convex optimization problem, implying guaranteed computational times.

The asymmetric and position/rate constraint problems proved to be extremely challenging ones. In short, it rapidly becomes difficult to maintain a high level of performance while providing guarantees. The added complexity of the constraints increases the difficulty of approximating the associated maximal invariant regions. In the case of position and rate constrained actuators this was remedied by using a convex optimization algorithm to increase the region of attraction for each value of the nonlinear gain. The concept of sub-controllable sets is particularly attractive because of their optimality, that is, they can provide finite time convergence and good performance. However, it is a challenging problem to extend them beyond the application to position constraints only. In this case, the problem is obtaining the best possible approximation to the actual controllable set.

Several questions and areas for further research exist. The immediate question is whether the methods presented here can be improved upon. In other words are there additional developments that will allow for better approximations of the maximal invariant sets. Is a performance enhancement like the one used for the position/rate constraint problem possible for the asymmetric problem? This ties in directly with the discussion on sub-controllable sets. That is, how do we obtain a differential equation for the evolution of state constrained sub-controllable sets? How do we construct an asymmetric controller based on sub-controllable sets? In the development of the asymmetric controller invertibility of the A matrix was assumed. Can this restriction be removed in certain cases, or all together? A further issue is the role of generalized design methods such as the one presented here. The application to the F/A-18 HARV shows the method is capable of comparison with the existing F/A-18 HARV control law. But what is the best use of the knowledge we have obtained? Does it represent a method usable for control systems design, or is it something like a fast prototyping tool? Because of its guarantees could it provide a backup, or redundant control system? Finally, real time implementation of optimal control strategies re-

quires guaranteed bounds on solution times. There is the possibility that the methods presented here could be used to bound the number of optimization steps needed to solve a receding horizon optimal control problem.

5.2 Convex Optimization for Aircraft Conflict Detection and Resolution

The second methodology applies to systems subject to more general state and control constraints. In essence it is the same as the first methodology. In other words the idea is always to approximate the admissible regions by convex sets. The selection of a control strategy can then be formulated as a convex optimization problem. This is presented through the aircraft conflict detection and resolution problem. It is an extremely important one that has even more of a requirement for guarantees than the nonlinear actuator problem. This is due to the fact the human lives are at risk and failure is unacceptable. The problem is approached from a two phase point of view. First conflicts are detected by means of a worst case analysis. This is accomplished through Linear Matrix Inequality feasibility problems, that provide a guaranteed indication of a conflict. Once this has been performed a conflict resolution method is proposed that can solve multiple aircraft conflicts. Unfortunately, the method becomes very complex for more than 3 or 4 aircraft because a "crossing-direction" must be specified for each aircraft pair. A possible solution to this problem is presented by formulation of the lower bound optimization problem and an examination of the null space of the resulting solution matrix. This does show promise for reducing the problem complexity. Again, computational times are guaranteed in all of this due to the convex optimization formulations.

Again, there are a wide variety of questions and avenues for research. First, is the more thorough investigation of the lower bound. The notion that somehow the lower bound optimization problem "knows" the best solution is irresistible. It is a challenging problem to determine if this is or is not true. Both a better theoretical and

statistical study need to be done here. Beyond this are the daunting implementation issues. These are several, including most importantly, guaranteed safety and the ability for real time computation.

A final question that combines much of this discussion is: How do we continue to increase or maintain guarantees while simultaneously delivering performance?

Bibliography

- [1] D. Delahaye and J. M. Alliot, Private Conversations, July 1997.
- [2] John Andrews, Private Conversations, Lincoln Laboratory, February 1997.
- [3] Final report of RTCA task force 3: Free Flight implementation. Washington DC, October 1995.
- [4] Special issue on control of systems with saturating actuators, *International Journal of Robust Nonlinear Control*, vol. 5, no. 5, 1995.
- [5] J. W. Andrews, J. C. Koegler, and K. D. Senne. IPC design validation and flight testing. Technical report, Lincoln Laboratory, MIT, 1978. Report No. FAA-RD-77-150.
- [6] K. J. Astrom and B. Wittenmark. *Computer Controlled Systems: Theory and Design*. Prentice Hall, 3rd edition, 1997.
- [7] H. Beh and G. Hofinger. Control law design of the experimental aircraft X-31A. In *19th ICAS Congress, Anaheim, CA.*, pages 541–549, September 1994.
- [8] A. Benzaouia and C. Burgat. Regulator problem for linear discrete-time systems with non-symmetrical constrained control. *Int. J. Control*, 48(6):2441–2451, 1988.
- [9] G. Bitsoris. Positively invariant polyhedral sets of discrete-time linear systems. *Int. J. Control*, 47(6):1727–1735, 1988.

- [10] G. Bitsoris and M. Vassilaki. Constrained regulation of linear systems. *Automatica*, 31(2):223–227, 1995.
- [11] F. Blanchini, F. Mesquine, and S. Miani. Constrained stabilization with an assigned initial condition set. *Int. J. Control*, 62(3):601–617, 1995.
- [12] F. Blanchini and S. Miani. Constrained stabilization of continuous-time linear systems. *Syst. Control Letters*, 28(2):95–102, 1996.
- [13] C. Boussios and E. Feron. Estimating the conservatism of Popov’s criterion. In *AIAA Guidance Navigation and Control Conf.*, San Diego, July 1996.
- [14] S. Boyd, L. El Ghaoui, E. Feron, and V. Balakrishnan. *Linear Matrix Inequalities in System and Control Theory*. SIAM, 1994.
- [15] S. Boyd and L. Vandenberghe. Convex optimization, 1996. Course Reader for EE364: Introduction to Convex Optimization with Engineering Applications.
- [16] B. Carpenter and J. Kuchar. Probability-based collision alerting logic for closely-spaced parallel approach. In *35th Aerospace Sciences Meeting and Exhibit*, Reno, January 1997. AIAA 97-0222.
- [17] F. L. Chernousko. *State estimation for dynamic systems*. CRC Press, 1994.
- [18] N. Durand, J. M. Alliot, and O. Chansou. Optimal resolution of en route conflicts. *Air Traffic Control Quarterly*, 3(3):139–161, 1995.
- [19] M. S. Eby. A self-organizational approach for resolving air traffic conflicts. *The Lincoln Laboratory Journal*, 7(2):239–253, 1994.
- [20] M. F. Friedman. Decision analysis and optimality in air traffic control conflict resolution. *Transportation Research Part B*, 22B(3):207–216, June 1988.
- [21] A. T. Fuller. In the large stability of relay and saturating control systems with linear controllers. *Int. J. Control*, 10(4):457–480, 1969.

- [22] P. Gahinet, A. Nemirovskii, A. J. Laub, and M. Chilali. *The LMI Control Toolbox*. MathWorks Inc., 1995.
- [23] V. M. Gavrilyako, V. I. Korobov, and G. M. Skylar. Designing a bounded control of dynamic systems in entire space with the aid of a controllability function. *Automation and Remote Control*, pages 1484–1490, 1987.
- [24] L. El Ghaoui, F. Delebecque, and R. Nikoukhah. *LMITool: A User-Friendly Interface for LMI Optimization*, 1995. Beta Version.
- [25] E. G. Gilbert. Linear control systems with pointwise-in-time constraints: What do we do about them? In *Proc. American Control Conf.*, page 2565, 1992.
- [26] E. G. Gilbert and K. T. Tan. Linear systems with state and control constraints: the theory and application of maximal output admissible sets. *IEEE Trans. Aut. Control*, 36(9):1008–1020, September 1991.
- [27] P. O. Gutman and M. Cwikel. Admissible sets and feedback control for discrete-time linear dynamical systems with bounded controls and states. *IEEE Trans. Aut. Control*, 31(4):373–376, April 1986.
- [28] P. O. Gutman and P. Hagander. A new design of constrained controllers for linear systems. *IEEE Trans. Aut. Control*, 30(1):22–33, 1985.
- [29] J. J. Harris and G. T. Black. F-22 control law development and flying qualities. In *AIAA Guidance Navigation and Control Conf.*, pages 155–168, San Diego, July 1996.
- [30] K. Havel and J. Husarcik. A theory of the tactical conflict prediction of a pair of aircraft. *Journal of Navigation*, 42(1):417–429, 1989.
- [31] R. A. Hess and S. A. Snell. Flight control system design with rate saturating actuators. *AIAA J. on Guidance, Control and Dynamics*, 20(1):90–96, January 1997.

- [32] P. Hou, A. Saberi, Z. Lin, and P. Sannuti. Simultaneous external and internal stabilization for continuous and discrete-time critically unstable linear systems with saturating actuators. In *Proc. American Control Conf.*, Albuquerque, June 1997. Submitted to *Automatica*.
- [33] V. A. Kamenetskii. Synthesis of bounded stabilizing control for an n-fold integrator. *Automation and Remote Control*, 52(6):770–775, 1991.
- [34] P. Kapasouris and M. Athans. Control systems with rate and magnitude saturation. In *Proc. IEEE Conf. on Decision and Control*, pages 3404–3409, Honolulu, 1990.
- [35] P. Kapasouris, M. Athans, and G. Stein. Design of feedback control systems for stable plants with saturating actuators. In *Proc. IEEE Conf. on Decision and Control*, pages 469–479, Austin, 1988.
- [36] D. H. Klyde, D. T. McRuer, and T. T. Myers. PIO analysis with actuator rate limiting. In *AIAA Guidance Navigation and Control Conf.*, pages 569–580, San Diego, July 1996.
- [37] V. A. Komarov. Design of constrained controls for nonautonomous linear systems. *Automation and Remote Control*, 45(10):1280–1286, 1984.
- [38] V. I. Korobov. A general approach to the solution of the bounded control synthesis problem in a controllability problem. *Math. USSR Sbornik*, 37(4):535–557, 1980.
- [39] M. V. Kothare, V. Balakrishnan, and M. Morari. Robust constrained model predictive control using linear matrix inequalities. *Automatica*, 32(10):1361–1379, 1996.
- [40] M. V. Kothare, P. J. Campo, M. Morari, and C. N. Nett. A unified framework for the study of anti-windup designs. *Automatica*, 30(12):1869–1883, 1994.

- [41] J. Krozel, M. E. Peters, and G. Hunter. Conflict detection and resolution for future air transportation management. Technical Report TR 97138-01, Seagull Technology, 1997.
- [42] J. K. Kuchar and L. Y. Yang. Survey of conflict detection and resolution modeling methods. In *AIAA Guidance Navigation and Control Conf.*, New Orleans, August 1997. AIAA-97-3732.
- [43] T. Lauvdal and T. I. Fossen. Semi-global results on stabilization of linear systems with input rate and magnitude saturations. In *AIAA Guidance Navigation and Control Conf.*, New Orleans, August 1997.
- [44] Z. Lin. Semi-global stabilization of linear systems with position and rate-limited actuators. *Syst. Control Letters*, 30:1–11, 1997.
- [45] Z. Lin, M. Pachter, S. Banda, and Y. Shamash. Feedback design for robust tracking of linear systems with rate limited actuators. In *AIAA Guidance Navigation and Control Conf.*, New Orleans, August 1997.
- [46] Z. Lin, M. Pachter, S. Banda, and Y. Shamash. Stabilizing feedback design for linear systems with rate limited actuators. to appear in *Control of Uncertain Dynamic Systems with Bounded Inputs*, eds. S. Tarbouriech and Germain Garcia, Lecture notes in Control and Information Sciences, Springer-Verlag, 1997.
- [47] D. Q. Mayne and W. R. Schroeder. Nonlinear control of linear systems. *Int. J. Control*, 60(5):1035–1043, 1994.
- [48] M. McConley, B. D. Appleby, M. A. Dahleh, and E. Feron. A control Lyapunov function approach to robust stabilization of nonlinear systems. Submitted to *IEEE Transactions on Automatic Control*, 1996.
- [49] A. Megretski. Output feedback stabilization with saturated control: making the input-output map L_2 bounded. In *Proc. 13th Triennial World Congress of IFAC*, volume D, pages 435–440, 1996.

- [50] P. K. A. Menon. Control theoretic approach to air traffic conflict resolution. In *AIAA Guidance Navigation and Control Conf.*, 1993. AIAA-93-3832-CP.
- [51] P. Miotto. *Fixed Structure Methods for Flight Control Analysis and Automated Gain Scheduling*. PhD thesis, Massachusetts Institute of Technology, 1997.
- [52] P. Miotto, J. Paduano, and J. Burken. Nonlinear F-18 simulator for MATLAB and SIMULINK. Technical Manual, Revision 0.0, 1996.
- [53] P. Miotto, J. M. Shewchun, E. Feron, and J. D. Paduano. High performance bounded control synthesis with application to the F18 HARV. In *AIAA Guidance Navigation and Control Conf.*, San Diego, July 1996.
- [54] Y. Nesterov and A. Nemirovsky. *Interior-point polynomial methods in convex programming*, volume 13 of *Studies in Applied Mathematics*. SIAM, Philadelphia, PA, 1994.
- [55] A. Packard, K. Zhou, P. Pandey, and G. Becker. A collection of robust control problems leading to LMI's. In *Proc. IEEE Conf. on Decision and Control*, December 1991.
- [56] R. A. Paielli and H. Erzberger. Conflict probability estimation for free flight. *AIAA J. on Guidance, Control and Dynamics*, 20(3):588–596, May 1997.
- [57] A. C. M. Ran and L. Rodman. On parameter dependence of solutions of algebraic Riccati equations. *Math. of Control, Signals, and Systems*, pages 269–284, 1988.
- [58] R. T. Rockafellar. *Convex Analysis and Optimization*. Pitman, Boston, 1982.
- [59] M. Rosenlicht. *Introduction to Analysis*. Dover, 1968.
- [60] L. Rundqwist and R. Hillgren. Phase compensation of rate limiters in JAS 39 Gripen. In *AIAA Guidance Navigation and Control Conf.*, pages 69–79, San Diego, July 1996. AIAA-96-3368.
- [61] A. Saberi, Z. Lin, and A. R. Teel. Control of linear systems with saturating actuators. *IEEE Trans. Aut. Control*, 41(3):368–378, 1996.

- [62] A. Saberi and A. A. Stoorvogel. Stabilization and regulation of linear systems with saturated and rate-limited actuators. In *Proc. American Control Conf.*, Albuquerque, June 1997.
- [63] M. G. Safonov and M. Athans. Gain and phase margins for multiloop LQG regulators. *IEEE Trans. Aut. Control*, 22(2):173–179, 1977.
- [64] W. E. Schmitendorf and B. R. Barmish. Null controllability of linear systems with constrained controls. *SIAM J. on Control and Optimization*, 18(4):327–345, July 1980.
- [65] J. M. Shewchun and E. Feron. High performance bounded control. In *Proc. American Control Conf.*, Albuquerque, June 1997.
- [66] R. A. Silverman. *Introductory Complex Analysis*. Dover, 1972.
- [67] R. Slattery and Y. Zhao. Trajectory synthesis for air traffic automation. *AIAA Guidance Navigation and Control Conf.*, 20(2):232–238, March 1997.
- [68] J.-J. E. Slotine and W. Li. *Applied Nonlinear Control*. Prentice Hall, 1991.
- [69] B. Sridhar and G. B. Chatterji. Computationally efficient conflict detection methods for air traffic management. In *Proc. American Control Conf.*, Albuquerque, 1997.
- [70] R. Suarez, J. Solis-Duan, and J. Alvarez. Stabilization of linear controllable systems by means of bounded continuous nonlinear feedback control. *Syst. Control Letters*, 23:403–410, 1994.
- [71] H. J. Sussmann, E. D. Sontag, and Y. Yang. A general result on the stabilization of linear systems using bounded controls. *IEEE Trans. Aut. Control*, 39(12):2411–2424, 1994.
- [72] H. J. Sussmann and Y. Yang. On the stabilizability of multiple integrators by means of bounded feedback controls. In *Proc. IEEE Conf. on Decision and Control*, pages 70–72, 1991.

- [73] M. Sznaier, R. Suarez, S. Miani, and J. Alvarez-Ramirez. Optimal l_∞ disturbance attenuation and global stabilization of linear systems with bounded control. Submitted to the Int. Journal of Robust and Nonlinear Control, 1997.
- [74] A. R. Teel. Global stabilization and restricted tracking for multiple integrators with bounded controls. *Syst. Control Letters*, 18:165–171, 1992.
- [75] C. Tomlin, G. J. Pappas, and S. Sastry. Conflict resolution for air traffic management: a case study in multi-agent hybrid systems. Preprint, 1996.
- [76] J. Van de Vegte. *Feedback Control Systems*. Prentice Hall, 2nd edition, 1990.
- [77] L. Vandenberghe and S. Boyd. *SP: Software for Semidefinite Programming*. Stanford University, 1994. Beta Version.
- [78] L. Vandenberghe and S. Boyd. Semidefinite programming. *SIAM Review*, 38(1):49–95, March 1996.
- [79] M. Vassilaki and G. Bitsoris. Constrained regulation of linear continuous-time dynamical systems. *Syst. Control Letters*, 13:247–252, 1989.
- [80] J. P. Wangemann and R. F. Stengel. Optimization and coordination of multi-agent systems using principled negotiation. In *AIAA Guidance Navigation and Control Conf.*, San Diego, July 1996. AIAA-96-3853.
- [81] G. F. Wredenhagen and P. R. Bélanger. Piecewise-linear LQ control for systems with input constraints. *Automatica*, 30(3):403–416, 1994.
- [82] G. F. Wredenhagen and P. R. Bélanger. Dynamic control of systems with asymmetric input constraints using interpolation functions. Preprint, 1995.
- [83] S. Wu and S. Boyd. *SDPSOL, A Parser/Solver for Semidefinite Programming and Determinant Maximization Problems with Matrix Structure*. Stanford University, May 1996.

- [84] L. Yang and J. Kuchar. Prototype conflict alerting logic for free flight. In *Proceedings of the 35th AIAA Aerospace Sciences Meeting and Exhibit*, January 1997.
- [85] K. Zeghal. Towards the logic of an airborne collision avoidance system which ensures coordination with multiple cooperative intruders. In *ICAS Proceedings*, pages 2208–2218, 1994. ICAS-94-8.6.4.